Atmospheric hydroperoxides in West Antarctica: links to stratospheric ozone and atmospheric oxidation capacity

Markus M. Frey[a,d], Richard W. Stewart[b], Joseph R. McConnell[c], Roger C. Bales[d]

[a]*Department of Hydrology and Water Resources, University of Arizona, 1133 E. North Campus Drive, Tucson AZ 85721, USA.*

[b]*Atmospheric Chemistry and Dynamics Branch, National Aeronautics and Space Administration (NASA) Goddard Space Flight Center (GSFC), Greenbelt, Maryland, USA.*

[c]*Desert Research Institute, Divison of Hydrologic Sciences, 2215 Raggio Parkway, Reno, NV 89512, USA.*

[d]*University of California, Merced, 4225 N. Hospital Road, Bldg 1200, Atwater, CA 95301, USA.*

Corresponding author:
Markus M. Frey
University of California, Merced
4225 N. Hospital Rd., Bldg. 1200
Atwater, CA-95301
mfrey@ucmerced.edu, phone: 209-205 8565, fax: 209-724 4459

Abstract

The troposphere above the West Antarctic Ice Sheet (WAIS) was sampled for hydroperoxides at 21 locations during 2-month-long summer traverses from 2000 to 2002, as part of US ITASE (International Transantarctic Scientific Expedition). First time quantitative measurements using an HPLC method showed that methylhydroperoxide (MHP) is the only important organic hydroperoxide occurring in the Antarctic troposphere, and that it is found at levels ten times those previously predicted by photochemical models. During three field seasons, means and standard deviations for hydrogen peroxide (H_2O_2) were 321±158 pptv, 650±176 pptv and 330±147 pptv. While MHP was detected, but not quantified in December 2000, levels in summer 2001 and 2002 were 317±128 pptv and 304±172.2 pptv. Results from firn air experiments and diurnal variability of the two species showed that atmospheric H_2O_2 is significantly impacted by a physical snow pack source between 76 and 90 °S, whereas MHP is not. We show strong evidence of a positive feedback between stratospheric ozone and H_2O_2 at the surface. Between November-27 and December-12 in 2001, when ozone column densities dropped below 220 DU (means in 2000 and 2001 were 318 DU and 334 DU, respectively), H_2O_2 was 1.7 times that observed in the same period in 2000 and 2002, while MHP was only 80% of the levels encountered in 2002. Photochemical box model runs suggest that NO and OH levels on WAIS are closer to coastal values, while Antarctic Plateau levels are higher, confirming that region to be a highly oxidizing environment. The modeled sensitivity of H_2O_2 and particularly MHP to NO offers the potential to use atmospheric hydroperoxides to constrain the NO background and thus estimate the past oxidation capacity of the remote atmosphere.

Index Terms: 0365 Atmospheric Composition and Structure: Troposphere: composition and chemistry; 0322 Atmospheric Composition and Structure: Constituent sources and sinks; 1610 Global Change: Atmosphere (0315, 0325); 0736 Cryosphere: Snow (1827, 1863); 0724 Cryosphere: Ice Cores (4932)

Keywords: hydrogen peroxide, methylhydroperoxide, Antarctica, air-snow exchange, stratospheric ozone, atmospheric oxidation capacity

1. Introduction

Atmospheric photooxidants are responsible for the removal of carbon monoxide (CO), methane (CH_4), nitrogen oxides (NO, NO_2), dimethyl sulfide (DMS), sulfur dioxide (SO_2) and halogenated compounds and thus control particle formation, the buildup of greenhouse gases and ultimately climate change. Hydroperoxides (ROOH) contribute to the oxidizing power of the troposphere [*Lee, et al.*, 2000], defined as the total burden of ozone (O_3), HO_x radicals and hydrogen peroxide (H_2O_2), and also constitute an important radical reservoir. There is increasing evidence that polar snow packs influence the overlying atmosphere by uptake and release of NO_x, organic acids, formaldehyde (HCHO) [*Dominé and Shepson*, 2002] and H_2O_2 [*Hutterli, et al.*, 2004; *Hutterli, et al.*, 2001]. Elevated HO_x levels at South Pole [*Mauldin, et al.*, 2001; *Mauldin, et al.*, 2004] and changes in ground level O_3 in relation to stratospheric O_3 depletion in spring [*Jones and Wolff*, 2003] show that snow-atmosphere interactions can alter the budget of atmospheric oxidants in the boundary layer. In addition, ice core records of H_2O_2 [*Anklin and Bales*, 1997; *Sigg and Neftel*, 1991] help constrain reconstructions of past atmospheric oxidation capacity, provided processes controlling deposition and preservation are understood [*McConnell, et al.*, 1997a].

In the presence of sunlight, water vapor and O_3, the short-lived OH radical is produced and converted into peroxyradicals through the oxidation of CO, CH_4 or other non-methane hydrocarbons:

$$CO + OH + O_2 \rightarrow CO_2 + HO_2 \quad \text{(R1)}$$

$$CH_4 + OH + O_2 \rightarrow H_2O + CH_3O_2 \quad \text{(R2)}$$

The main photolytic source of ROOH is the combination of peroxyradicals:

$$HO_2 + HO_2 \rightarrow H_2O_2 + O_2 \quad \text{(R3)}$$

$$RO_2 + HO_2 \rightarrow ROOH + O_2 \quad \text{(R4)}$$

However, competing reactions with NO, which represent also the core of photochemical O_3 production in the troposphere, can suppress the formation of hydroperoxides depending on the level of NO present [*Kleinmann*, 1991; *Stewart*, 1995]:

$$NO + HO_2 \rightarrow NO_2 + OH \quad \text{(R5)}$$

$$NO + CH_3OO\ (+ O_2) \rightarrow NO_2 + HCHO + HO_2 \quad \text{(R6)}$$

Observations from South Pole during the polar day show that H_2O_2 first increases with increasing NO, and decreases once NO levels exceed 100 pptv [*Hutterli, et al.*, 2004].

With methane as the only significant organic peroxy radical precursor at remote sites, methylhydroperoxide (MHP, CH_3OOH) is expected to be the dominant organic peroxide in

Antarctica. Photolysis and attack by the OH radical are the main photochemical sinks for hydroperoxides.

$$H_2O_2 + h\nu \rightarrow 2\,OH \qquad (R7),\ (\lambda < 355\ nm)$$

$$CH_3OOH + h\nu\ (+O_2) \rightarrow HCHO + OH + HO_2 \qquad (R8),\ (\lambda < 360\ nm)$$

$$H_2O_2 + OH \rightarrow H_2O + HO_2 \qquad (R9)$$

$$CH_3OOH + OH \rightarrow CH_3OO + H_2O \qquad (R10)$$

Wet deposition affects the highly water soluble H_2O_2 and less so higher organic peroxides. This follows from the fact that the Henry's Law constant for MHP is only 0.1% of that for H_2O_2 [*Lind and Kok*, 1994]. Dry deposition of ROOH above snow and ice surfaces can also impact atmospheric levels, as model studies at South Pole showed [*Hutterli, et al.*, 2004]. It has to be noted though that deposition is reversible for these gases and changes in temperature of the surface snowpack drive a cycle of emission and uptake until the top layer is buried by additional accumulation and disconnected from further exchange [*Hutterli, et al.*, 2001; *Wolff and Bales*, 1996].

The only Antarctic hydroperoxide data available are summer observations of H_2O_2 at South Pole [*Hutterli, et al.*, 2004; *McConnell, et al.*, 1997b], spot measurements from a traverse in Dronning Maud Land (73-76°S) [*Fuhrer, et al.*, 1996] and observations over various seasons at the coastal Neumayer Station [*Jacob and Klockow*, 1993; *Riedel, et al.*, 2000].

The main goal of our study was to understand factors controlling the photochemistry of hydroperoxides in the background atmosphere above Antarctica, away from anthropogenic and biogenic emission sources and across a wide gradient of temperature, accumulation rate, latitude and elevation. There are two motivations. First, hydroperoxides are 'diagnostic tools' of atmospheric oxidation capacity (e.g. *Riedel, et al.*, 2000 and, *Lee, et al.*, 2000), however a quantitative link to polar HO_x radical levels is lacking. Second, a quantitative understanding linking ROOH, oxidant levels, solar radiation and climate is essential to interpreting variability in ROOH from ice cores in terms of atmospheric change.

2. Methods

We measured concentrations of atmospheric hydroperoxides in ambient and firn interstitial air above the West Antarctic Ice Sheet (WAIS) during three 2-month-long ground traverses from 2000 to 2002 (Figure 1; Table 1). Sinks and sources of ROOH were also investigated, including radiative conditions, atmospheric properties and snow-atmosphere exchange. Results were integrated using a photochemical box model.

Traverse routes connected low-elevation WAIS regions with the cold and dry East Antarctic Plateau (Table 1). Each site was occupied typically for 1-4 days and atmospheric experiments were carried out 500 m upwind from the main camp in a Scott Polar tent (2000) and a heated Weatherhaven™ shelter mounted onto a sledge (2001-2002). Mixing ratios of atmospheric hydroperoxides were monitored continuously using a 2-channel method, with total peroxides determined in channel 1 [e.g. *Jacobi, et al.*, 2002] and the amount and speciation of individual peroxides measured in channel 2 (Figure 2). For each channel ambient air was drawn through an insulated, heated PFA (¼" I.D.) intake line (typically 1.4 STP-L min^{-1}) mounted at ~1 m above the snow.

Peroxides were scrubbed from the air stream into aqueous solution and analyzed using a fluorescence detection method [*Jacobi, et al.*, 2002]. A number of instrument upgrades were made following the 2000 field season to improve performance. Separation of H_2O_2 and organic hydroperoxides was achieved using HPLC [*Kok, et al.*, 1995; *Lee, et al.*, 1995], involving automatic injection of a 912 µl sample every 10 minutes, with post-column chemistry and detection as in channel 1. Instrument response was calibrated 1-2 times per day with commercially available H_2O_2 and MHP standards synthesized in our lab [after *Rieche and Hitz*, 1929].

Firn interstitial air was sampled at 6 sites by periodically alternating a single intake line between ambient and firn air every ~30 minutes over a 4-6 h period. To sample firn air a hole was cored to ~10 cm depth, the intake line inserted and snow packed around the line.

Channel 2 output was linearly interpolated to the sample times of channel 1 (1 value per 10 s) and used to correct channel 1 for contributions of organic peroxides. Collection efficiencies (CE) for MHP determined in the lab at 5.8 °C and 13.0 °C to be 0.86 and 0.75, respectively, were in agreement with Henry's Law (equilibrium constants adopted from *Lind and Kok*, 1994). Therefore data were processed with CE calculated according to Henry's equilibrium using coil temperature and pressure. Coil temperature was controlled to within 0.1 K and coil pressure estimated based on observed ambient pressure. The variability in ambient pressure on ITASE (range 690-840 mbar) would lead to overestimates of CE by up to ~4%, if not accounted for. Liquid flow rates were corrected for evaporation occurring in the coil scrubbers with corrections being generally on the order of 5%.

The limit of detection (LOD), defined as 3 times the baseline standard deviation, for H_2O_2 from channel 1 was 50 pptv during the first two field seasons and 30 pptv during the last one. The precision was usually better than 20 pptv. MHP measurements from channel 2 had a LOD of <150 pptv in 2001 and <30 pptv during 2002 with precisions amounting to 60 pptv.

Overall accuracy of the measurements for both species is better than 20%, where the largest contributions to the overall error originate from the uncertainties in liquid flow rates and coil pressure (MHP only). Most H_2O_2 data reported are from channel 1, with H_2O_2 from channel 2 only used in the case of data gaps.

Firn and ambient air formaldehyde (HCHO) levels (24-hr averages) were determined using Sep-Pak® DNPH-Silica Cartridges (Waters, Milford, MA) containing acidified dinitrophenylhydrazine reagent coated on a silica sorbent [*Kleindienst, et al.*, 1998]. Sample air (2200 to 3000 L) was pumped through an ozone scrubber and then through the cartridge, which was mounted in an insulated housing and kept above freezing. Intake lines were also insulated and heated, as noted above for ROOH. After sampling sample cartridges (including blanks) were sealed, wrapped in aluminum foil and transported frozen back to the US for analysis.

Standard meteorological variables, including air temperature, atmospheric pressure and wind speed, were measured at each site, with surface UV-A irradiance (315-378 nm) added in 2001 and 2002.

Balloon soundings using RS-80 (Vaisala, Helsinki, Finland) radiosondes attached to a helium-filled balloon were carried out frequently in order to determine the thermal structure and ozone profile of the atmospheric boundary layer. During a typical sounding experiment, the balloon was frequently raised and lowered over a time period of ~1 hr at a rate of 1-2 m s^{-1} using a 1000 m long tether and an electric winch. Air temperature, atmospheric pressure and relative humidity were transmitted to a ground station consisting in radio antenna, receiver and a computer as a data logger. In 2001 ozone was measured at the ground level in between tethered balloon launches. In 2002 surface ozone was determined continuously at each site using a 2B Technologies (Golden, CO) ozone monitor [*Helmig, et al.*, 2002]. Instruments were usually placed in the heated tent and a Teflon sample line was passed to the outside and mounted 1 m above the snow about 2 m away from the tent.

We used the NASA-Goddard Flight Center (GSFC) point photochemical model to integrate and evaluate measurements [*Stewart*, 2004], with modifications necessary to simulate the Antarctic boundary layer. The model chemistry contains a basic NO_x-HO_x-O_x scheme including methane, ethane and ethene oxidation, but with the addition of a simplified DMS oxidation scheme [*Sander and Crutzen*, 1996]. There are 30 variable species undergoing 70 reactions. In addition to chemical production and loss, several species are assumed to have physical sources and sinks, most importantly NO, H_2O_2, and HCHO. These were varied sinusoidally with the solar elevation angle, the maximum flux occurring at the maximum solar elevation angle. Fluxes were converted to source values by assuming they are distributed through

a 250 m boundary layer. Deposition velocities are mostly from *Hauglustaine et al.* [1994], except that the rate for HCHO was taken for the same as that for CH_3CHO.

Model runs were constrained with time series of atmospheric chemistry and meteorology data. Total ozone burden was extracted for each location from the Total Ozone Mapping Spectrometer (TOMS) dataset (ftp.toms.gsfc.nasa.gov). Data gaps were filled using scaled Dobson meter measurements from South Pole. CO, CH_4 and surface-ozone data were available from the NOAA CMDL air sampling network station at South Pole (ftp.cmdl.noaa.gov). Based on a comparison with ozone measurements during ITASE, the surface-ozone time series from McMurdo-Arrival Heights on the coast were considered representative for the West Antarctic Ice Sheet, while time series from South Pole were taken for sites on the Antarctic Plateau. AWS (Automatic Weather Station) data from Byrd Station (http://uwamrc.ssec.wisc.edu/) and the South Pole (ftp.cmdl.noaa.gov) provided the meteorological input of air temperature, atmospheric pressure and humidity.

3. Results

3.1 Atmospheric concentrations of peroxides

Means, standard deviations and ranges for H_2O_2 during ITASE 2000, 2001 and 2002 were 321±158 (<50-888) pptv, 650±176 (141-1212) pptv and 330±147 (<30-918) pptv, respectively (Figure 3). For ITASE 2001 and 2002 MHP levels were 317±128 (<150-1125) pptv and 304±172.2 (<30-1025) pptv, respectively. MHP mixing ratios in ambient air were in general as high as or lower than H_2O_2, with the exception of measurements during a storm event at site 02-2 (Figure 3c).

MHP, the only higher organic peroxide detected, typically contributed 12-15% to the total fluorescence signal in channel 1. After this correction H_2O_2 concentrations from channel 1 compared well with results from the HPLC method. During ITASE 2000 MHP was detected in the ambient air at three sites (00-4, 00-5 and 00-7), but low signal to noise ratios and baseline drifts did not allow quantification.

While MHP showed only low frequency changes over several days, H_2O_2 exhibited a diurnal cycle at many sites during times when wind speeds were low (0-5 m s^{-1}). The daily maximum H_2O_2 levels were usually in phase with or lagged air temperature maxima by up to 4 hours. The amplitude of daily cycles, when recognizable, ranged from 130 up to 380 pptv. The daily amplitude of solar elevation angle (SEA) decreases with southern latitude and is zero at the South Pole. Correlations between daily amplitudes of either H_2O_2 or air temperature and latitude

showed no significant trend at the 99% level, but at locations south of 80°S H_2O_2 diurnal cycles were less frequent and disappeared on the Antarctic Plateau all together.

Mean atmospheric levels of MHP at each site show a significant decrease between 76° and 90° S, from a high of 491±296 pptv to a low of 102±41 pptv (Figure 4b). It is notable that the range and standard deviation of MHP concentrations also show a statistically significant, linear decrease with more southern latitudes. The latitudinal trend of H_2O_2 is more complicated, ranging from a high of 803±150 pptv to a low of 230±56 pptv with ITASE 2000 observations in general lower than in 2001 at similar latitudes (Figure 4a). The contribution of MHP to total peroxides (Figure 4c), ranged from 0.04 to 0.98 with a mean of 0.39±0.15. The highest mean value of 0.62 was observed at 02-2, the only site with a value above 0.5.

3.2 Firn air measurements

A total of 8 sets of firn air measurements were carried out, mostly between local noon and local midnight (median solar time 16:40). In 6 of the 8 sets, firn-air H_2O_2 was 1.3-3.5 times ambient air concentrations (Table 2) with gradients between the upper 10 cm of snow and the atmosphere ranging between 0.1 and 13.3 ppbv/m. These gradients assume that the shallow layer above the snow surface is well mixed and H_2O_2 levels between the air-snow interface and measurement height of 1 m are the same. Note that firn and ambient air measurements were not concurrent and therefore ratios assume that neither firn nor ambient air concentrations changed significantly over two subsequent ~20 min sampling intervals of firn and ambient air. In 2 cases, at site 01-5 and 02-2, ambient levels of H_2O_2 were higher than in the firn. On the other hand, MHP mixing ratios exhibited no significant differences, partly due to increased scatter during the sampling of firn air.

All firn-air results are from channel 1. When firn air was sampled HPLC data showed large scatter and H_2O_2 values 2-3 times those from channel 1, and were therefore discarded.

Our firn air experiments were generally done on calm days; wind speeds were close to zero at site 01-5 and less than 4 m/s at the other sites, where measured (02-1 and 02-5). Movement of H_2O_2 molecules in the open firn space is reduced by sorption on the media and tortuosity effects. Effective molecular diffusivities D_{eff} were estimated after *Schwander et al.*[1989] based on measured atmospheric pressure, air temperature and snow density and ranged between a low of 8.99 x 10^{-6} m^2s^{-1} at site 01-5 and a high of 1.35 x 10^{-5} m^2s^{-1} at the South Pole, which is equivalent to a reduction by up to 30% when compared to the free air diffusivities. Characteristic diffusion times t across distance d of 1 cm following the Einstein-Smoluchowski relationship $t = 0.5 \times d^2 D_{eff}^{-1}$ were 4-6 s. These estimates are higher than the 1 s modeled

previously by *Hutterli et al.* [2003], but still are only 10% (50%) of South Pole (Siple Dome) translation times due to forced ventilation (modeled vertical ventilation velocities at wind speeds of ~3 m s^{-1} were 1 mm s^{-1} at Siple Dome [*Albert*, 2002] and 0.2 mm s^{-1} at South Pole [*McConnell, et al.*, 1998]). It is thus assumed that molecular diffusion rather than forced ventilation due to pressure pumping induced by horizontal airflow across a rough snow surface dominated vertical fluxes across the snow-air interface.

Mean snow pack emissions of H_2O_2 were 7.0 x 10^{11} molecules $m^{-2}s^{-1}$ ranging from 1.8 x 10^8 to 2.6 x 10^{12} molecules $m^{-2}s^{-1}$, while at sites 01-5 and 02-2 net deposition fluxes were on average 3.1 x 10^{11} molecules $m^{-2}s^{-1}$ (Figure 5). The mean HCHO flux from the data sets at Byrd and 02-5 was 9.4 x 10^{10} molecules $m^{-2}s^{-1}$. A linear regression between gradients and mean air temperatures during the experiments showed a weak correlation ($r^2 = 0.18$), but significant at the 99% level. Other factors, however, such as latitude and snow concentrations of H_2O_2 integrated over the top 30 cm exhibited no statistical relationship either to fluxes or to gradients (Figure 5).

3.3 Modeling results

The photochemical box model was run at two sites representing two extrema of conditions covered by ITASE. First, Byrd is a site at lower elevation and latitude with noticeable diurnal cycles of SEA (13 to 33°) and air temperature (–17 to –11°C) in December (air temperatures measured on-site compared well to the 19-yr mean diurnal cycle for Byrd in December, derived from AWS data). Second, South Pole is a site with constant SEA and consequently no diurnal cycle; air temperatures averaged –25.9°C during the first week of January 2003. Stratospheric ozone concentrations had already recovered from the annual springtime depletion when field measurements were carried out, and amounted to 332 Dobson Units (DU) above Byrd and 272 DU above the South Pole.

The model included dry deposition of H_2O_2 and MHP with rates set initially to 0.32 and 0.01 cm s^{-1}, respectively. The value of 0.32 cm s^{-1} for H_2O_2 suggested by *Hauglustaine et al.* [1994] translates into a deposition rate of 1.3 x 10^{-5} s^{-1} assuming a boundary layer height of 250 m, which is of the same order of magnitude as the first-order heterogeneous removal rate of 9.3 x 10^{-5} s^{-1} derived for South Pole [*Slusher, et al.*, 2002]. The chosen box height of 250 m in the model was justified by the range of observed mixing layer heights. Most of our balloon soundings, including a total of 117 measured vertical profiles at ITASE 2001 and 2002 sites, showed very stable surface inversion layers during the coldest time of the solar day of 20 to 490 m (mean 132 m) vertical extension followed by the development of a mixed layer during local morning to late afternoon hours, when the surface was warming, ranging from 13 m to 354 m.

With parameters set to their standard values, model output of H_2O_2, MHP and HCHO was 18%, 14%, 56% at Byrd and 4%, 7% and 11% at South Pole when compared to observed site means (Figure 6). In a second set of model runs maximum observed diffusional fluxes of H_2O_2 and HCHO were introduced into the model to simulate a heterogeneous snowpack source. In addition, the MHP production rate from $CH_3O_2 + HO_2$ was increased within its estimated range of uncertainty [*DeMore, et al.*, 1997]. Deposition velocities for HCHO, MHP, and H_2O_2 were also reduced, but with negligible effect at times corresponding to the observations. Model output matched site means of atmospheric mixing ratios within the observed 1σ variability, however depending on the NO background chosen, fit was optimal either for H_2O_2 and HCHO or for H_2O_2 and MHP, but not for all 3 chemical species (Figure 6).

4. Discussion

4.1 Relative hydroperoxide levels

Mean December H_2O_2 levels in 2000 and 2002 were 1.6 times the average concentrations determined on the coast at Neumayer Station (200 vs. 325 pptv) [*Riedel, et al.*, 2000] while the range of both data sets compares well (~30-900 pptv). The coastal mean values, however, covered data from September 1997 to March 1998 and February 1999, including low spring and fall values. Our average H_2O_2 mixing ratios on the Antarctic Plateau at sites 02-4, 02-5 and the South Pole (230-290 pptv) were similar to December 1995 (180-250 pptv) [*McConnell, et al.*, 1997b] and 2000 (280 pptv) [*Hutterli, et al.*, 2004] levels at the South Pole. It is striking that mean H_2O_2 concentrations above WAIS during December 2001 were twice those during the other field seasons (650 vs. 325 pptv) and maximum values were the highest ever reported from Antarctica (1200 pptv). These levels, however, were still lower than concentrations observed at Summit, Greenland by *Bales et al.* [1995] (500-2000 pptv), *Jacobi et al.* [2002] (650 pptv) and *Frey and Bales* [1999] (400-3800 pptv).

When compared to the only other existing study, MHP mixing ratios from 2001 and 2002 were 60% higher than levels at Neumayer (310 vs. 190 pptv) [*Riedel, et al.*, 2000], while again those included values from the entire sun lit season. It is interesting to note that MHP at the South Pole in the first week of January 2003 (100 pptv) was ten times that predicted by photochemical steady state model runs for the ISCAT campaign in December 2000 [*Hutterli, et al.*, 2004].

Our MHP:(MHP+H_2O_2) ratios of 0.39±0.15 (range 0.04 to 0.98) were on average lower than reported from Neumayer of 0.57±0.26 (range 0.1 to 1.0) [*Riedel, et al.*, 2000], but in the range of values found in the mid latitudes of the North and South Atlantic where ratios of 0.32±0.12 [*Weller, et al.*, 2000] and 0.48±0.14 [*Slemr and Tremmel*, 1994] were reported. The

magnitude and temporal variability of these ratios are thought to reflect preferential depletion of H_2O_2 by dry and wet deposition, which may also be why ratios in coastal Antarctica are higher than in continental air. The highest ratios measured on ITASE, during a storm event at site 02-2, were not due to depleted H_2O_2 but rather a consequence of elevated MHP (Figures 3c and 4c). Wind speeds during the storm exceeded 18 m/s and created a zone of blowing snow extending vertically several tens of meters and decreasing visibility to below 10 m. MHP levels were highly variable reaching up to 600 pptv, when H_2O_2 remained around ~200 pptv. After wind speeds decreased to 13 m/s the snow suspension settled and MHP dropped to 200 pptv. Surface ozone during the storm showed a distinct drop from 17 ppbv down to 11 ppbv and recovered 24 hrs later to 14 ppbv, when there was no layer of blowing snow. We eliminated evaporating snow crystals in the intake line as a cause for this observation since the atmospheric H_2O_2 signal was not affected. Photochemical experiments at Summit, Greenland showed that OH concentrations in ambient air were consistently higher than model predictions, especially during episodes of high winds and blowing snow, suggesting that an unknown mechanism converts HO_2 into OH [*Huey, et al.*, 2004]. Though the true reactions involved are not understood we suspect that elevated MHP during the storm at 02-2 also reflects a shift in HO_x partitioning.

The surprisingly high levels of organic hydroperoxides have consequences for the accuracy of current atmospheric analytical methods. The bulk peroxide fluorescence detection method (here channel 1) was applied in the past to determine absolute H_2O_2 levels under the assumption that higher organic peroxides can be neglected at remote polar sites such as Central Greenland [*Bales, et al.*, 1995; *Sigg, et al.*, 1992]. However, our findings show that in West Antarctica the presence of MHP would lead on average to H_2O_2 overestimates by up to 15%, higher than previously assumed for Summit, Greenland [*Sigg, et al.*, 1992]. Since MHP lacks the diurnal cycle exhibited by H_2O_2, MHP:(H_2O_2+MHP) ratios increase during the coldest time of the day and would lead to potential overestimates of H_2O_2 of, in our case, ~50%. Therefore, H_2O_2 concentrations determined with the bulk method during times when the sun is at its minimum elevation during the polar day should, if uncorrected, be interpreted with caution.

4.2 Factors controlling the variability of ROOH

Both photochemical and physical sinks and sources as well as local meteorological conditions (atmospheric water vapor, air temperature, surface UV radiation) affect the variability of trace chemical species in the atmosphere. These not only differed across the ITASE sites, but also varied during the measurement periods. Therefore our results contain both temporal and spatial variability (Figures 3 and 4).

Summer air temperatures dropped from –12 to –27°C in moving from WAIS onto the Antarctic Plateau, largely as a function of altitude, r^2=0.67 (Figure 7a). Lapse rates across all 3 ITASE seasons were sub-adiabatic at –8.45 °K/km. Specific humidities closely followed air temperature, r^2=0.83 (Figure 7b), as expected from the temperature dependence of water vapor pressure, and show that the air above WAIS contains 3 times the atmospheric moisture as does that above the Antarctic Plateau. Wind speeds were in general highly variable, but during the ITASE 2002 season they appeared to be less so and lower, often below 5 m/s on the Antarctic Plateau (Figure 7c). At latitudes north of 85 °S measured surface ozone levels remained below 20 ppbv most of the time, while they were significantly higher on the Antarctic Plateau (sites 02-3, 02-4 and 02-5) reaching a maximum at the South Pole (Figure 7d). Low surface ozone on the coast and elevated levels at South Pole during the summer are also observed in time series from Arrival Heights-McMurdo (77.8 °S 166.8 °E) and South Pole over the past decade (data from ftp.cmdl.noaa.gov). The main precursors of hydroperoxides in the remote troposphere, CH_4 and CO, are well mixed across the entire study area, as seen by comparison of data sets from Halley Station (75.6 °S 26.6 °W), Palmer Station (64.8 °S 64.1 °W) and South Pole, and declined between November and January, from 1.71 ppbv to 1.70 ppbv and 55 ppbv to 38 ppbv, respectively (ftp.cmdl.noaa.gov).

SEA at solar noon varied between 36° and 23° across all ITASE seasons and daily amplitudes dropped from 28° at site 01-6 to 0° at the South Pole. As a consequence, daily amplitudes of air temperature at Byrd were 5.7 °K, with no diurnal pattern at South Pole. Measured surface UV-A radiation tracked the variability in SEA (r^2=0.96; data not shown). Unfortunately, our measurements did not extend to the UV-B region of the solar spectrum, where the absorption of H_2O_2, MHP and O_3 is strongest and, as expected, UV-A and O_3 burden showed no significant relationship. Therefore we used the Tropospheric Ultraviolet-Visible (TUV) radiation model version 4.1 (http://www.acd.ucar.edu/TUV) [*Madronich and Flocke*, 1998] to calculate surface UV-B (280-315 nm) and photolysis rates of H_2O_2, MHP and O_3 taking into account current location, elevation and local total ozone burden under the assumption of clear-sky conditions and a surface albedo typical for the Antarctic ice sheet of 0.9 [*King and Turner*, 1997]. Daily means of modeled surface UV-B were highest during ITASE 2001, up to double levels in 2000 and 2002 at the same time of year in similar regions (Figure 8 d-f). Daily amplitudes were large (Figure 8 d-e) and decreased to zero towards the South Pole (Figure 8 f). Fluctuations in the O_3 burden clearly dominate seasonal SEA changes in driving the variability of surface UV-B, as can be seen by comparing the results to model simulations where O_3 column density is held constant at 290 DU (dotted line in Figure 8 d-f). At the end of November 2001, O_3 burden

dropped within 7 days by 70 DU, while the model predicted a 5-fold increase of surface UV-B in addition to the seasonal SEA effect.

H_2O_2 and MHP are both positively correlated with specific humidity (Figure 9a and e) as water vapor is a significant precursor for both. High UV-B also gives high H_2O_2 mixing ratios (Figure 9 b). However, MHP was not sensitive to UV-B (Figure 9 f). While H_2O_2 levels dropped off with increasing surface ozone concentrations on the Polar Plateau (Figure 9c), MHP increased with O_3 between 10 and 20 ppbv. Above 20 ppbv MHP levels were suppressed, less variable, with median values below 150 pptv. These trends of both hydroperoxide species are consistent with an increase in net production of surface O_3 through reactions R5 and R6 at the expense of hydroperoxide formation. Additional NO is released from the snow pack after photolysis of NO_3^- stored in the upper snow layer. Indeed, elevated surface O_3 levels observed at the South Pole suggested photochemical production rates of 2.2 to 3.6 ppbv/day [*Crawford, et al.*, 2001] and NO levels were surprisingly high [*Davis, et al.*, 2004b], in part due to snow emissions of NO_x from NO_3^- photolysis [*Honrath, et al.*, 1999]. During periods of high NO H_2O_2 levels were suppressed [*Hutterli, et al.*, 2004].

Local meteorological conditions affect vertical and horizontal transport and thus the variability of chemical species. Higher wind speeds, at least up to 10 m s^{-1}, resulted in lower H_2O_2 (Figure 9d), while MHP and wind speed show no significant correlation (Figure 9h); an exception was the storm event described above. While this is not definitive, it is consistent with the fact that H_2O_2 emissions out of the snow pack are mixed into the boundary layer and thus diluted through turbulent transport much more efficiently during periods of higher wind speeds than during calm days, as was observed in the case of NO during the ISCAT campaign [*Davis, et al.*, 2004a].

Snow pack emissions of H_2O_2 and HCHO at the South Pole in December 2000 were determined to be on the order of 1 x 10^{13} and 2 x 10^{12} molecules $m^{-2}s^{-1}$, respectively [*Hutterli, et al.*, 2004]. Our gradients were smaller, resulting in diffusional fluxes about 10% of those from ISCAT 2000 [*Hutterli, et al.*, 2004] (Figure 5). Differences are due in part to dilution of firn air with an unknown amount of ambient air during sampling, making reported values lower limits. At these reduced rates the reservoir of H_2O_2 in the snow phase is not limiting, e.g. at maximum emission flux, average H_2O_2 snow concentrations of 4.4 μM and a mean snow density of 370 kg m^{-3} in the upper 10 cm of snow pack [*Frey et al.*, in preparation] it would take ~1.2 yr to deplete H_2O_2 completely from the upper snow layer.

The observed large diurnal cycle of H_2O_2 is most likely caused by the same reversible temperature driven exchange mechanism as at Summit, Greenland, where diurnal cycles have been explained by net emission during the day and net deposition during the night [*Hutterli, et*

al., 2001]. Even though no decrease in amplitude with more southern latitude was observed, our findings that H_2O_2 and air temperature amplitudes show a weak correlation and no diurnal cycles were detected south of 85 °S are consistent with a decrease in variability of air temperature and snowpack emissions at the more southern latitudes.

A significant physical MHP source in the surface is unlikely, given that no diurnal cycle was observed and that MHP remained below the detection limit of 7 ppbw in all samples from 1 m snow pits collected at ITASE 2000 sites [*Frey et al.*, in preparation]. Previous attempts to find MHP down to a stated threshold of 0.1 ppbw in an Antarctic ice core at Law Dome failed as well [*Gillett, et al.*, 2000].

The contribution of the snow pack to boundary layer photochemistry also depends strongly on atmospheric dynamics and the vertical extent of the planetary boundary layer. For example, at site 02-4 ('Hercules Dome') H_2O_2 concentrations dropped between 25-Dec 0:00 UTC and 25-Dec 3:00 UTC from levels above 400 pptv down to ~220 pptv. Balloon profiles from 24-Dec 21:35 UTC and 25-Dec 2:45 UTC showed the existence of a mixed layer of 120–150 m vertical extent, remaining virtually unchanged over the same time period, and therefore dilution effects due to an expansion of that layer can be excluded. Air temperatures dropped from –18 to –26 °C, leading to a change in H_2O_2 consistent with decreased snow pack emissions or even net deposition during lower temperatures. Back trajectories (see below) showed that air originating from the Weddell Sea sector from 4 days prior arrived with only marginal vertical movements within the planetary boundary layer at 02-4 at the same time.

At Neumayer Station advection of marine air was responsible for sporadic increases in ROOH during the polar night when the photochemical production of peroxides is shut down [*Riedel, et al.*, 2000]. Also inland locations such as South Pole can be influenced by influx of marine air [*Swanson, et al.*, 2004]. Daily back trajectories calculated for all ITASE seasons with the NOAA HYSPLIT model [http://www.arl.noaa.gov/ready; *Draxler and Rolph*, 2003] show that air masses originating in the Amundsen, Bellingshausen or Weddell Sea sector can reach central locations on the West Antarctic Ice Sheet within less than ~3 days, with the air at ground level moving along the topography. According to the same trajectories air masses are also advected frequently through katabatic flow from the Antarctic Plateau down slope to lower elevations of WAIS. We compared these transport times with atmospheric lifetimes τ of H_2O_2 and MHP with respect to reaction with OH and photolysis using $\tau_{h2o2} = (k_{R9}\,[OH] + k_{R7})^{-1}$ and $\tau_{MHP} = (k_{R10}\,[OH] + k_{R8})^{-1}$. Reaction rates from *Atkinson et al.* [1997] were extrapolated to conditions at ITASE locations and photolysis rates calculated with the TUV model. The lifetimes of H_2O_2 and MHP averaged over all field seasons were 49 hr and 63 hr, assuming coastal levels of OH of 0.5 x

10^5 molecules cm^{-3} [*Jefferson*, 1998] and decreased to 25 and 34 hr, when the ISCAT 2000 mean for OH of 2.1 x 10^6 molecules cm^{-3} at South Pole [*Mauldin, et al.*, 2004] was used. Including dry deposition decreased ranges to 14 and 57 hr in the low and 11 and 33 hr in the high OH scenario.

Thus it is unlikely that H_2O_2 at locations in the interior of Antarctica in summer time, even during meteorological situations that facilitate fast transport from the coast, is impacted by distant off-continent source regions. In the case of MHP long range transport might play a role at WAIS locations closer to the coast due to the smaller sensitivity to heterogeneous removal and therefore longer lifetimes, however our observations lack any sudden changes in concentration to support this.

4.3 Stratospheric ozone

The high H_2O_2 and lower MHP concentrations above WAIS during 2001 can be explained by 3 factors: a) change in relative abundance of atmospheric precursors CO, CH_4 or water vapor, b) variability of the physical heterogeneous snow pack source, and c) changes in surface UV-B, with corresponding impacts on the HO_x-NO_x cycle and the ROOH budget. In order to evaluate interannual differences of ROOH levels we compared 15-day periods in December 2000, 2001 and 2002 when measurements were carried out at locations with similar features (Table 3). By comparing equal time periods of different years we exclude seasonal variations of the solar elevation angel as a contributing factor and expect UV-B to change only as a function of location and stratospheric ozone. Mean UV-B calculated with a constant ozone overhead column of 290 DU is indeed comparable between the 15-day periods of all 3 seasons, with the slightly lower value for 2002 reflecting the fact that 02-40, Byrd and 02-1 are located at more southern latitudes (Table 3). Between November-27 and December-12 in 2001 H_2O_2 was 70% higher than during the same time period in 2000 and 2002, while MHP was 80% the levels encountered in 2002 (Table 3).

It is unlikely that atmospheric precursors of H_2O_2 are responsible for much of the interannual differences. While CH_4 mixing ratios in all 3 years were almost identical, December 2000 had 6-8 ppbv less CO than 2001 and 2002. However, no effect on mean H_2O_2 is obvious, since December 2000 levels were comparable to the mean of December 2002 (Table 3). Atmospheric moisture was 80% higher in 2002 when compared to 2001, while the concurrent change in H_2O_2 was opposite of what is expected if the difference was driven by humidity changes. MHP, however, followed the pattern in atmospheric moisture.

Systematically higher air temperatures in combination with stable atmospheric stratification and recent deposition prior to air sampling could potentially lead to increases in

H_2O_2 levels as a consequence of temperature driven release from the snow pack [*Hutterli, et al.*, 2001]. Conversely, regularly occurring fog events could lower H_2O_2 levels through net deposition, as suggested to be the primary reason for below average H_2O_2 levels during a 3-week period at Summit, Greenland [*Hutterli, et al.*, 2004; *Jacobi, et al.*, 2002]. However, wind speeds showed no significant difference between seasons, mean air temperatures were lower when H_2O_2 was high (Table 3), and fog events were observed occasionally, but were not systematically more frequent on the ITASE 2000 and 2002 traverses.

This leaves systematic differences in surface UV-B as the leading cause for differences in H_2O_2. Previous model studies predicted that enhanced surface UV-B increases ozone photolysis, leading to enhanced OH and H_2O_2 [*Fuglestvedt, et al.*, 1994]. Ozone column densities were low in December 2001 and dropped below the ozone-hole-defining threshold of 220 DU [*Newman, et al.*, 2004] above most of the West Antarctic Ice Sheet, including sites 01-1, 01-2 and 01-3 (Figures 8 and 10). In the present case a decrease in O_3 column density can increase production of H_2O_2 through two mechanisms: enhanced ozone photolysis and increase of photolytically induced snow pack emissions of NO in a low-NO_x regime, where both species are positively correlated. This is consistent with the low MHP in December 2001, which according to our model sensitivity study should decrease rapidly as NO concentrations rise.

With high surface UV-B in 2001 (Figure 8e) photolysis rates of ROOH and ozone are expected to increase, with the latter showing large positive perturbations when ozone burden is low (Figure 11, 4th row). The first direct observations at South Pole during ISCAT 2000 revealed that decreases in overhead O_3 column density were accompanied by increases in $j(O_3 \rightarrow O(^1D)+O_2)$ and OH concentrations [*Mauldin, et al.*, 2004]. Ozone photolysis rates calculated with the TUV model during times of low O_3 burden are up to 5 times the observed values during the first week of December 2000 at South Pole, and maximum values $>5 \times 10^{-5}$ s^{-1} are comparable to photolysis rates calculated for mid latitude locations (non-polluted sky at sea level, SEA of 0° and surface albedo 0.03, [*Jacobson*, 1999]). Therefore, enhanced primary production of OH through $O(^1D)+H_2O_{(g)} \rightarrow OH + OH$ after ozone photolysis followed by R1 appears to be one likely cause for additional H_2O_2 formation, more than outweighing increased H_2O_2 loss by photolysis. The slow decrease in observed surface ozone levels during the comparison periods in 2001 and 2002 (Figure 11, 5th row) points also to a regime of net destruction of O_3.

The change in NO_x chemistry due to increased surface radiation and nitrate photolysis in the snow results in a net increase in OH and H_2O_2. Surface radiation changes related to the ozone hole drive the rate of nitrate photolysis in the upper snowpack enough to increase NO_x emissions and lead to a net production of ozone [*Jones and Wolff*, 2003], possibly explaining elevated

surface ozone levels observed at the South Pole during summer [*Crawford, et al.*, 2001] starting in the late 1970s after the onset of the ozone hole. Box model simulations for the ISCAT 2000 data set suggest that elevated and highly variable OH and HO_2+RO_2 are a direct result of equally high and variable levels of nitrous oxide. The reason for high OH is that NO is efficiently cycling HO_2 into OH. Correlations between NO and OH or H_2O_2 both showed a positive relationship up to a threshold of ~100 pptv of NO [*Hutterli, et al.*, 2004; *Mauldin, et al.*, 2004]. Beyond that H_2O_2 production is suppressed. This hypothesis is supported by the observation of enhanced surface O_3 on the Antarctic Plateau indicating net O_3 production (Figure 11, 5th row) and the lower MHP in 2001 (Table 3). MHP formation is suppressed at lower NO levels than is H_2O_2 and shows a rapid decline as NO increases (see below).

There is a time lag between changes in O_3 burden and the response in H_2O_2 at the surface (Figure 11), most likely due to the fact that the system is not in photochemical steady state. Indicators of a low NO_x regime are low surface ozone above WAIS and low NO levels reported from the coast [*Jefferson*, 1998; *Jones, et al.*, 1999]. Since our box model scales the NO source as the inverse square of the cosine of solar zenith angle and does not include at this point nitrate photolysis it comes to no surprise that modeled OH (not shown) and H_2O_2 (Figure 11, 2nd row) fail to show a significant increase during low O_3-burden episodes. Modeled H_2O_2 in 2001 is slightly higher than in 2002 and shows a small positive change after overhead ozone has passed through a minimum clearly not capturing the increase indicated by observations. ROOH observed at Neumayer Station during the period of stratospheric ozone depletion in 1997 showed mixing ratios comparable to typical winter levels and no obvious change [*Riedel, et al.*, 2000]. However, in the Neumayer data set a large increase in H_2O_2 occurs between day of year 310 and 320 (1997), right around the time where surface O_3 shows higher variability and tendency to increases as well. This is consistent with *Jones and Wolff* [2003], who found that the impact of change in UV-B radiation on nitrate photolysis and subsequently elevated NO becomes important later in the sunlit season at higher solar elevation angels.

4.4 Atmospheric oxidation capacity

Since calculated hydroperoxides in our box model runs were highly sensitive to the NO_x background (not measured) the NO source term in the model was set to achieve modeled ambient NO levels within the range of existing measurements in Antarctica. Mean coastal NO levels reported from Neumayer Station [*Jones, et al.*, 1999] and Palmer Station on the Antarctic Pensinsula [*Jefferson*, 1998] were less than 10 pptv, while high values were found at the South

Pole, averaging 133 and 244 pptv for Dec. 15-31 in 2000 and 1998, respectively [*Davis, et al.*, 2004b].

The sensitivity study showed that in a low NO_x regime (Byrd), H_2O_2 increases linearly with NO and after reaching a maximum at 10 pptv drops off quickly (Figure 12a) due to the competing conversion of HO_2 into OH by NO (R5). The decrease in MHP at higher NO is even more pronounced, since two reaction channels consume respective precursors HO_2 and CH_3OO at the same time, R5 producing again more OH and R6 forming HCHO. According to this model it is hard to sustain elevated MHP at the high NO mixing ratios observed at the South Pole, since MHP decreases rapidly at NO levels rising beyond 40 pptv at the South Pole (Figure 12b). Predictions of NO (OH) levels based on optimum model runs, including physical sources of H_2O_2 and HCHO, were 10 pptv (8.9×10^5 molecules cm^{-3}) at Byrd and 42 pptv (2.4×10^6 molecules cm^{-3}) at South Pole, respectively. Thus within the 1σ range the modeling suggests that a combination of our observations of H_2O_2, MHP and HCHO consistently constrain the NO_x background. As can be seen from Figure 12 MHP is the limiting species due to its high sensitivity to NO changes. Since NO_x is controlling the oxidizing capacity in the troposphere above the ice sheet, as seen by the close relationship between NO and OH (Figure 12), we consider this to be a quantitative link between ROOH, HCHO and current atmospheric oxidation capacity.

The modeled HO_x-NO_x chemistry at Byrd appears to be close to the composition of the atmosphere on the coast [*Jefferson*, 1998; *Jones, et al.*, 1999], while the constrained simulations for South Pole are qualitatively in agreement with the ISCAT results and further confirm that the Antarctic Plateau is a unique atmospheric environment of high oxidizing power. However, it should be noted that NO levels above 100 pptv, as observed during ISCAT 2000, are clearly not in agreement with the relatively high MHP measured on ITASE. Since a physical snowpack source of MHP is unlikely, other photochemical reactions involving organic trace gases can potentially lead to increased MHP. Even at a remote location as the interior of the Antarctic there are appreciable amounts of organic molecules in the snow; e.g. the TOC content of South Pole snow samples was found to be similar to Arctic snow from Summit, Greenland or Alert, Nunavut [*Grannas, et al.*, 2004]. Ethene emissions from the snowpack, as observed at Alert, Nunavut [*Bottenheim, et al.*, 2002], could contribute to MHP production through gas phase ozonolysis. Lab experiments provided evidence that reaction of ozone with alkenes can yield alkylperoxides including MHP under dry conditions [*Gab, et al.*, 1995; *Horie, et al.*, 1994]. Another possible mechanism is the photooxidation of acetone, $CH_3(CO)CH_3 + h\nu + O_2 \rightarrow CH_3OO + CH_3C(O)O_2$, leading to the formation of additional methylperoxy radicals. Under low NO conditions more MHP is then produced through R4. The trace gas acetone was found to be emitted from high

latitude snowpack as results from the ALERT 2000 campaign show [*Guimbaud, et al.*, 2002]. However, formation mechanisms for organic hydroperoxides are in general still poorly understood and further field measurements including other possible organic precursor species are required to understand MHP sources in the remote environment.

5. Conclusions

First, it is important to note that the US ITASE ground traverse served as an excellent research platform for an extensive atmospheric sampling program in remote West Antarctica, providing a unique data set of atmospheric observations across latitudes, similar to measurement campaigns on oceanic vessels. Our findings from spatially distributed spot measurements of summer levels of ROOH above the West Antarctic Ice Sheet indicate that atmospheric water vapor, actinic flux and consequently ozone column density, and, in the case of H_2O_2, a heterogeneous snow pack source, are the main factors controlling atmospheric concentrations. The upper snow pack between 76 and 90 °S is a net source of H_2O_2, at least during the latter half of the solar day in summer and probably over the full diel cycle for many months, while a physical source of MHP is less likely to play an important role. First time quantitative measurements using HPLC show that MHP is the only important organic hydroperoxide occurring in the Antarctic troposphere, and is of similar concentration to H_2O_2 in the absence of enhanced surface UV-B from stratospheric O_3 depletion. We show strong evidence for a positive feedback between stratospheric ozone depletion and surface levels of H_2O_2 by comparing differences in atmospheric moisture content, air temperature and photolysis rates from a radiation transfer model calculation. The difference of H_2O_2 above WAIS in the low O_3-burden year 2001 compared to the 2000 and 2002 seasons is significant. Enhanced surface UV-B radiation upon depletion in ozone column density affects H_2O_2 mixing ratios through increased ozone photolysis and increases in NO_x following nitrate photolysis in the upper snow pack. This finding will impact the interpretation of century scale records of H_2O_2, which are currently being developed from shallow cores recovered at all ITASE locations [*Frey, et al.*, 2004].

The US ITASE traverse across WAIS provided a link between the two atmospheric environments, the coast and the Antarctic Plateau, where tropospheric chemistry in summer has been characterized before. Photochemical box model runs constrained by observations of H_2O_2, MHP and HCHO suggest that NO and OH levels on WAIS are closer to coastal values, while Antarctic Plateau levels are higher, confirming the unique nature of that region as a highly oxidizing environment. This also implies that the positive feedback on H_2O_2 from higher surface UV-B due to a thinning stratospheric ozone layer should be more pronounced in the WAIS region

where NO_x levels are low. The modeled sensitivity of H_2O_2 and particularly MHP to NO_x reveals the potential use of atmospheric hydroperoxides to constrain the NO background and to evaluate the current and also, using ice core reconstructions, past strength of a photolytic NO source in the snow pack. Since NO itself is tightly linked to the oxidation power of the atmosphere in remote regions, this link is expected to narrow upper and lower limits on atmospheric HO_x. Future work will need to characterize organic precursors from the snow pack and improve the model parameterization of NO flux from nitrate photolysis in the snow pack in order to capture the large observed increase in H_2O_2.

Acknowledgements.

This work was supported by the National Science Foundation's Office of Polar Programs (OPP-9814810, OPP-9811875 and OPP-9904294). Special thanks to S. Oltmans, B. Johnson from NOAA Climate Monitoring and Diagnostics Laboratory (Boulder, CO) for providing ozone instruments, radio sondes and training, B. Youngman for helping with ozone measurements and balloon soundings during ITASE 2002, J. Kahl (University of Wisconsin, Madison, WI) for providing winch and tether, D. Bell-Oudry for performing HPLC analysis of the DNPH cartridges at the University of Arizona and to Ratheon Polar Services and the U.S. ITASE field team for providing logistics and field support. We also gratefully acknowledge the NOAA Air Resources Laboratory (ARL) for the provision of the READY website (http://www.arl.noaa.gov/ready.html) used in this publication. Any opinions, findings, and conclusions or recommendations expressed in this material are those of the author(s) and do not necessarily reflect the views of the National Science Foundation.

References

Albert, M. R. (2002), Effects of snow and snow ventilation on sublimation rates, *Annals of Glaciology*, *35*, 52-56.

Anklin, M., and R. C. Bales (1997), Recent increase in H_2O_2 concentration at Summit, Greenland, *Journal of Geophysical Research*, *102*, 19099-19104.

Atkinson, R., D. L. Baulch, R. A. Cox, R. F. Hampson Jr., J. A. Kerr, M. J. Rossi, and J. Troe (1997), Evaluated kinetic, photochemical and heterogeneous data for atmospheric chemistry, *Journal of Physical Chemistry Reference Data, Supplement V*, 521-1011.

Bales, R. C., J. R. McConnell, M. V. Losleben, M. H. Conklin, K. Fuhrer, A. Neftel, J. E. Dibb, J. D. W. Kahl, and C. R. Stearns (1995), Diel variations of H_2O_2 in Greenland: A discussion of the cause and effect relationship, *Journal of Geophysical Research*, *100*, 18661-18668.

Bottenheim, J. W., H. Boudries, P. C. Brickell, and E. Atlas (2002), Alkenes in the Arctic boundary layer at Alert, Nunavut, Canada, *Atmospheric Environment*, *36*, 2585-2594.

Crawford, J. H., D. D. Davis, G. Chen, M. Buhr, S. Oltmans, R. Weller, L. Mauldin, F. Eisele, R. Shetter, B. Lefer, R. Arimoto, and A. Hogan (2001), Evidence for photochemical production of ozone at the South Pole surface, *Geophysical Research Letters*, *28*, 3641-3644.

Davis, D., G. Chen, M. Buhr, J. Crawford, D. Lenschow, B. Lefer, R. Shetter, F. Eisele, L. Mauldin, and A. Hogan (2004a), South Pole NOx Chemistry: an assessment of factors controlling variability and absolute levels, *Atmospheric Environment*, *38*, 5375-5388.

Davis, D. D., F. Eisele, G. Chen, J. Crawford, G. Huey, D. Tanner, D. Slusher, L. Mauldin, S. Oncley, and D. Lenschow (2004b), An overview of ISCAT 2000, *Atmospheric Environment*, *38*, 5363-5373.

DeMore, W. B., S. P. Sander, D. M. Golden, R. F. Hampson, M. J. Kurylo, C. J. Howard, A. R. Ravishankara, C. E. Kolb, and M. J. Molina (1997), Chemical Kinetics and Photochemical Data for Use in Stratospheric Modeling, JPL-Publication 97-4, Jet Propulsion Laboratory, Pasadena, CA.

Dominé, F., and P. B. Shepson (2002), Air-snow interactions and atmospheric chemistry, *Science*, *297*, 1506-1510.

Draxler, R. R., and G. D. Rolph (2003), HYSPLIT (HYbrid Single-Particle Lagrangian Integrated Trajectory) Model access via NOAA ARL READY Website (http://www.arl.noaa.gov/ready/hysplit4.html).

Frey, M. M., and R. C. Bales (1999), Impact of solar radiation and temperature on atmospheric H_2O_2 variations in and above snow at Summit, Greenland, *Eos, Transactions, American Geophysical Union*, *80*, F198.

Frey, M. M., J. R. McConnell, E. Hanna, and R. C. Bales (2004), First high resolution, century-scale ice core records of hydrogen peroxide from West Antarctica: Contribution of accumulation variability, *SCAR*, *28*, Abstract S21/P09.

Fuglestvedt, J. S., J. E. Jonson, and I. S. A. Isaksen (1994), Effects Of Reductions In Stratospheric Ozone On Tropospheric Chemistry Through Changes In Photolysis Rates, *Tellus Series B-Chemical And Physical Meteorology*, *46*, 172-192.

Fuhrer, K., M. Hutterli, and J. R. McConnell (1996), Overview of recent field experiments for the study of the air-snow transfer of H_2O_2 and HCHO, in *Chemical Exchange between the Atmosphere and Polar Snow, NATO ASI Series, Vol. I 43*, edited, pp. 307-318, Springer-Verlag, Berlin Heidelberg.

Gab, S., W. V. Turner, S. Wolff, K. H. Becker, L. Ruppert, and K. J. Brockmann (1995), Formation Of Alkyl And Hydroxyalkyl Hydroperoxides On Ozonolysis In Water And In Air, *Atmospheric Environment*, *29*, 2401-2407.

Gillett, R. W., T. D. van Ommen, A. V. Jackson, and G. P. Ayers (2000), Formaldehyde and peroxide concentrations in Law Dome (Antarctica) firn and ice cores, *Journal Of Glaciology*, *46*, 15-19.

Grannas, A. M., P. B. Shepson, and T. R. Filley (2004), Photochemistry and nature of organic matter in Arctic and Antarctic snow, *Global Biogeochemical Cycles*, *18*, doi:10.1029/2003GB002133.

Guimbaud, C., A. M. Grannas, P. B. Shepson, J. D. Fuentes, H. Boudries, J. W. Bottenheim, F. Domine, S. Houdier, S. Perrier, T. B. Biesenthal, and B. G. Splawn (2002), Snowpack processing of acetaldehyde and acetone in the Arctic atmospheric boundary layer, *Atmospheric Environment*, *36*, 2743-2752.

Hauglustaine, D. A., C. Granier, G. P. Brasseur, and G. Megie (1994), The importance of atmospheric chemistry in the calculation of radiative forcing on the climate system, *Journal of Geophysical Research*, *99*, 1173-1186.

Helmig, D., J. Boulter, D. David, J. W. Birks, N. J. Cullen, K. Steffen, B. J. Johnson, and S. J. Oltmans (2002), Ozone and meteorological boundary-layer conditions at Summit, Greenland, during 3-21 June 2000, *Atmospheric Environment*, *36*, 2595-2608.

Honrath, R. E., M. C. Peterson, S. Guo, J. E. Dibb, P. B. Shepson, and B. Campbell (1999), Evidence of NO_x Production within or upon Ice Particles in the Greenland snowpack, *Geophysical Research Letters*, *26*, 695-698.

Horie, O., P. Neeb, S. Limbach, and G. K. Moortgat (1994), Formation Of Formic-Acid And Organic Peroxides In The Ozonolysis Of Ethene With Added Water-Vapor, *Geophysical Research Letters*, *21*, 1523-1526.

Huey, G., S. Sjostedt, D. Tanner, J. Dibb, G. Chen, B. Lefer, J. Peischl, L. M. Hutterli, N. Blake, D. Blake, A. Beyersdorf, and T. Ryerson (2004), Measurements of OH and HO_2 + RO_2 at Summit / Greenland, *Eos Trans. AGU, Fall Meet. Suppl.*, *85*, A22C-02.

Hutterli, M. A., J. R. McConnell, R. C. Bales, and R. W. Stewart (2003), Sensitivity of hydrogen peroxide (H_2O_2) and formaldehyde (HCHO) preservation in snow to changing environmental conditions: Implications for ice core records, *Journal of Geophysical Research*, *108*, doi:10.1029/2002JD002528.

Hutterli, M. A., J. R. McConnell, G. Chen, R. C. Bales, D. D. Davis, and D. H. Lenschow (2004), Formaldehyde and hydrogen peroxide in air, snow and interstitial air at South Pole, *Atmospheric Environment*, *38*, 5439-5450.

Hutterli, M. A., J. R. McConnell, R. W. Stewart, H. W. Jacobi, and R. C. Bales (2001), Impact of temperature-driven cycling of hydrogen peroxide (H_2O_2) between air and snow on the planetary boundary layer, *Journal of Geophysical Research*, *106*, 15395-15404.

Jacob, P., and D. Klockow (1993), Measurements of hydrogen peroxide an Antarctic ambient air, snow and firn cores, *Fresenius Journal of Analytical Chemistry*, *346*, 429-434.

Jacobi, H.-W., M. M. Frey, M. A. Hutterli, R. C. Bales, O. Schrems, N. J. Cullen, K. Steffen, and C. Koehler (2002), Measurements of hydrogen peroxide and formaldehyde exchange between the atmosphere and surface snow at Summit, Greenland, *Atmospheric Environment*, *36*, 2619-2628.

Jacobson, M. Z. (1999), *Fundamentals of Atmospheric Modeling*, 656 pp., Cambridge University Press.

Jefferson, A. (1998), OH photochemistry and methane sulfonic acid formation in the coastal antarctic boundary layer, *Journal of Geophysical Research*, *103*, 1647-1656.

Jones, A. E., G. Weller, A. Minikin, E. Wolff, W. T. Sturges, H. P. McIntyre, S. R. Leonard, O. Schrems, and S. Bauguitte (1999), Oxidized nitrogen chemistry and speciation in the Antarctic troposphere, *Journal of Geophysical Research*, *104*, 21355-21366.

Jones, A. E., and E. W. Wolff (2003), An analysis of the oxidation potential of the South Pole boundary layer and the influence of stratospheric ozone depletion, *Journal of Geophysical Research*, *108*, doi:10.1029/2003JD003379.

King, J. C., and J. Turner (1997), *Antarctic Meteorology and Climatology*, 409 pp.

Kleindienst, T. E., E. W. Corse, F. T. Blanchard, and W. A. Lonneman (1998), Evaluation of the performance of DNPH-coated silica gel and C 18 cartridges in the measurement of formaldehyde in the presence and absence of ozone, *Environmental Science & Technology*, *32*, 124-130.

Kleinmann, L. I. (1991), Seasonal Dependence of Boundary Layer Peroxide Concentration: The Low and High NO_x Regimes, *Journal of Geophysical Research*, *96*, 20721-20733.

Kok, G. L., S. E. McLaren, and T. Staffelbach (1995), HPLC determination of atmospheric organic hydroperoxides, *Journal of Atmospheric and Oceanic Technology*, *12*, 282-289.

Lee, M., B. G. Heikes, and D. W. O'Sullivan (2000), Hydrogen peroxide and organic hydroperoxide in the troposphere: a review, *Atmospheric Environment*, *34*, 3475-3494.

Lee, M., B. C. Noone, D. W. O'Sullivan, and B. G. Heikes (1995), Method for the collection and HPLC analysis of hydrogen peroxide and C1 and C2 Hydroperoxides in the atmosphere, *Journal of Atmospheric and Oceanic Technology*, *12*, 1060-1170.

Lind, J. A., and G. L. Kok (1994), Correction to "Henry's law determinations for aqueous solutions of hydrogen peroxide, methylhydroperoxide, and peroxyacetic acid", *Journal of Geophysical Research*, *99*, 21119.

Liu, H., K. Jezek, B. Li, and Z. Zhao (2001), Radarsat Antarctic Mapping Project digital elevation model version 2, edited, Boulder, CO: National Snow and Ice Data Center. Digital media.

Madronich, S., and S. Flocke (1998), The role of solar radiation in atmospheric chemistry, in *Handbook of Environmental Chemistry*, edited by P. Boule, pp. 1-26, Springer-Verlag, Heidelberg.

Mauldin, R. L., F. L. Eisele, D. J. Tanner, E. Kosciuch, R. Shetter, B. Lefer, S. R. Hall, J. B. Nowak, M. Buhr, G. Chen, P. Wang, and D. Davis (2001), Meaurements of OH, H_2SO_4, and MSA at the South Pole during ISCAT, *Geophysical Research Letters*, 3629-3632.

Mauldin, R. L., E. Kosciuch, B. Henry, F. L. Eisele, R. Shetter, B. Lefer, G. Chen, D. Davis, G. Huey, and D. Tanner (2004), Measurements of OH, HO_2+RO_2, H_2SO_4, and MSA at the South Pole during ISCAT 2000, *Atmospheric Environment*, *38*, 5423-5437.

McConnell, J. R., R. C. Bales, R. W. Stewart, A. M. Thompson, M. R. Albert, and R. Ramos (1998), Physically based modeling of atmosphere-to-snow-to-firn transfer of H_2O_2 at South Pole, *Journal of Geophysical Research, 103*, 10561-10570.

McConnell, J. R., R. C. Bales, J. R. Winterle, H. Kuhns, and C. R. Stearns (1997a), A lumped parameter model for the atmosphere-to-snow transfer function for hydrogen peroxide, *Journal of Geophysical Research, 102*, 26,809.

McConnell, J. R., J. R. Winterle, R. C. Bales, A. M. Thompson, and R. W. Stewart (1997b), Physically based inversion of surface snow concentrations of H_2O_2 to atmospheric concentrations at South Pole, *Geophysical Research Letters, 24*, 441-444.

Newman, P. A., S. R. Kawa, and E. R. Nash (2004), On the size of the Antarctic ozone hole, *Geophysical Research Letters, 31*, doi:10.1029/2004GL020596.

Rieche, A., and F. Hitz (1929), Ueber Monomethyl-hydroperoxyd, *Berliner Deutsche Chemische Gesellschaft, 62*, 2458-2474.

Riedel, K., R. Weller, O. Schrems, and G. Koenig-Langlo (2000), Variability of tropospheric hydroperoxides at a coastal surface site in Antarctica, *Atmospheric Environment, 34*, 5225-5234.

Sander, R., and P. J. Crutzen (1996), Model study indicating halogen activation and ozone destruction in polluted air masses transported to the sea, *Journal of Geophysical Research, 101*, 9121-9138.

Schwander, J., H. Oeschger, and C. C. Langway (1989), The transformation of snow to ice and the occlusion of gases, in *The Environmental Record in Glaciers and Ice Sheets*, edited, pp. 53-67, John Wiley.

Sigg, A., and A. Neftel (1991), Evidence for a 50% increase in H_2O_2 over the past 200 years from a Greenland ice core, *Nature, 351*, 557-559.

Sigg, A., T. Staffelbach, and A. Neftel (1992), Gas phase measurements of hydrogen peroxide in Greenland and their meaning for the interpretation of H_2O_2 records in ice cores, *Journal of Atmospheric Chemistry*, *14*, 223-232.

Slemr, F., and H. G. Tremmel (1994), Hydroperoxides In The Marine Troposphere Over The Atlantic-Ocean, *Journal Of Atmospheric Chemistry*, *19*, 371-404.

Slusher, D., G. Huey, D. Tanner, G. Chen, D. Davis, M. Buhr, J. B. Nowak, F. Eisele, E. Kosciuch, R. L. Mauldin, B. Lefer, R. Shetter, and J. Dibb (2002), Measurements of pernitric acid at the South Pole during ISCAT 2000, *Geophysical Research Letters*, *29*, doi:10.1029/2002GL015703.

Stewart, R. W. (1995), Dynamics of the low to high NO_x transition in a simplified tropospheric photochemical model, *Journal of Geophysical Research*, *100*, 8929-8943.

Stewart, R. W. (2004), The annual cycle of hydrogen peroxide: Is it an indicator of chemical instability? *Atmospheric Chemistry And Physics*, *4*, 933-946.

Swanson, A. L., D. D. Davis, R. Arimoto, P. Roberts, E. L. Atlas, F. Flocke, S. Meinardi, F. Sherwood Rowland, and D. R. Blake (2004), Organic trace gases of oceanic origin observed at South Pole during ISCAT 2000, *Atmospheric Environment*, *38*, 5463-5472.

Weller, R., O. Schrems, A. Boddenberg, S. Gab, and M. Gautrois (2000), Meridional distribution of hydroperoxides and formaldehyde in the marine boundary layer of the Atlantic (48°N-35°S) measured during the Albatross campaign, *Journal of Geophysical Research*, *105*, 14401-14412.

Wolff, E. W., and R. C. Bales (1996), *Chemical Exchange between the Atmosphere and Polar Snow*, 675 pp., Springer Verlag, Berlin - Heidelberg.

Figure captions

Figure 1. WAIS map (based on Antarctic Digital Data Base v4.1 http://www.add.scar.org/) overlying the RAMP DEM [*Liu, et al.*, 2001] showing traverse routes of the US component of the International Transantarctic Scientific Expedition (US ITASE; details of the multi-disciplinary expedition at http://www.ume.maine.edu/USITASE/) in 2000-2002 and the 21 locations of atmospheric chemistry observations.

Figure 2. Schematic of 2-channel peroxide detector employed on ITASE; shown are air pumps (P), actuated injection valve (V), excitation source (Ex) and photo-multiplier tubes (PMT1 & 2).

Figure 3. Mixing ratios of H_2O_2 (black symbols) and CH_3OOH (grey symbols) from 3 ITASE seasons observed during the month of December in 2000 (a.), 2001 (b.) and 2002 (c.). H_2O_2 is reported as 10 min averages, while the plotted MHP data represent single chromatograms, each one of them representing a ~5 min average of sampled air. Note that as the season progressed the measurement location changed as well, as indicated by the site index attached to each group of data. Data gaps are time periods when the ground traverse was in transition to a different site and no measurements were done.

Figure 4. Site averages of atmospheric mixing ratios of H_2O_2 (a) and MHP (b) and ratios of MHP to total peroxide (c) as a function of latitude. Symbols are means with error bars indicating one standard deviation and shaded areas the full range of measurements.

Figure 5. Estimates of H_2O_2 fluxes based on measured gradients between ambient and firn interstitial air are plotted as a function of latitude. Bars represent the mean and error bars 1 σ uncertainty. Note that at site 01-5 and 02-4 two sets of measurements are shown.

Figure 6. Comparisons between observations and photochemical box model estimates of atmospheric H_2O_2, MHP and HCHO mixing ratios for Byrd (a-c) and South Pole (e-g). Calculated NO background values are plotted as well for both sites (d,h). Various model scenarios include: 1) a base case with standard reaction rates and no heterogeneous fluxes for ROOH and HCHO (grey lines) and 2) multiple runs with reaction rates optimized for MHP production, emission fluxes of H_2O_2 and HCHO included and the NO source set for different backgrounds in December (blue and red lines). Black symbols are observed mean concentrations at each site with error bars indicating the 1σ uncertainty range, while symbols in grey represent

10 min averages of measured H_2O_2 and MHP. No DNPH results were available from South Pole, instead one 24 hr run from site 02-5 was used for comparison with no uncertainty range (g).

Figure 7. Correlation plots of observed and calculated environmental parameters on ITASE: a. air temperature vs. elevation with the black line illustrating the linear trend (slope –8.45 K/m, r^2 = 0.67), b. observed specific humidity q_v (symbols and error bars correspond to median, 25th and 75th percentile of each bin) vs. air temperature. Also shown is potential q_v at RH=100% (25th and 75th percentile as grey lines), c. wind speed vs. latitude and d. surface ozone vs. latitude. Symbols and error bars in a., c. and d. represent mean and 1σ uncertainty at each site and individual field seasons are color coded: ITASE 2000 (blue), ITASE 2001 (black) and ITASE 2002 (red). All meteorological and surface ozone data used are 10 min averages from December/January of the respective year (note that neither humidity nor surface ozone were measured in 2000).

Figure 8. Panels a-c show daily ozone column densities from TOMS during each field season above the location of the ITASE traverse on the same dates. Panels d-f show calculated surface UV-B (280-315 nm), where the black line represents daily means and the area shaded in grey illustrates the amplitude between solar noon and midnight; surface UV-B radiation was also calculated for ozone column densities fixed at a constant 290 DU (dotted black line).

Figure 9. Correlation plots of binned ROOH observations: (a./.e) H_2O_2/MHP vs. specific humidity q_v, (b./f.) H_2O_2/MHP vs. calculated surface UV-B radiation (280-315 nm), (c./g.) H_2O_2/MHP vs. surface ozone and (d./h.) H_2O_2/MHP vs. wind speed. Symbols and error bars represent median values and inner quartiles (25th and 75th percentiles). All data used are 10 min averages in December 2001, 2002 and early January 2003 (wind speed and UV-B correlation plots contain also December 2000 data).

Figure 10. Spatial distributions of total ozone above Antarctica are compared between December 2000 (Panel a.), 2001 (Panel b.) and 2002 (Panel c.). Images show data recovered by the Earth Probe TOMS instrument (http://toms.gsfc.nasa.gov/ozone). White areas represent data gaps.

Figure 11. Atmospheric H_2O_2 and related parameters are shown from 2000, 2001 and 2002, each column representing one season of measurements. Areas shaded in grey highlight the comparison period November-27 - December-12 (Table 3). In row 1 daily column densities of ozone are plotted against time (grey symbols represent Byrd, while the black symbols take into account the

current position of the ITASE traverse on the ice sheet). The second row shows 10 minute (grey symbols) and 24 hour averages (black symbols) of observed H_2O_2. Plotted are also simulated H_2O_2 mixing ratios in 2001 and 2002 from the optimized fit to observations at Byrd in 2002 (black line). The third row illustrates the variability of specific humidity (10 minute and 24 hr averages plotted as grey and black symbols, respectively; no data available from 2000). Calculated daily averages of photolysis rates for O_3 (black symbols) and H_2O_2 (grey symbols) are shown in the fourth row, and surface O_3 measurements from ITASE2001 and 2002 are plotted in the fifth row.

Figure 12. Sensitivities of calculated H_2O_2, CH_3OOH and HCHO to increasing NO background levels are shown for a. Byrd (29.11.02-7.12.02) and b. South Pole (2.01.03-5.01.03). Symbols represent output of individual box model runs for H_2O_2 (circles), MHP (grey triangles) and HCHO (squares). Observation ranges, defined as the mean plus and minus 1σ, are shown as shaded areas with solid, broken and dotted border lines for H_2O_2, CH_3OOH and HCHO respectively. Note that at South Pole only one data point for HCHO is available (see text). Panels c. and d. illustrate the relationship across the same model runs between calculated NO and OH radical concentrations at Byrd and South Pole.

Tables

Table 1. Locations of atmospheric chemistry observations

Site	lat/ long, °S/ °W	elev, m	T[a], °C	Dates
00-1	79.38/ 111.23	1791	-13.7	11/27 – 12/6/00
00-2	78.73/ 111.50	1675	-15.0	12/7 – 12/9/00
00-3	78.42/ 115.92	1741	-16.7	12/10 – 12/13/00
00-4	78.08/ 120.08	1697	-15.0	12/14 – 12/17/00
00-5	77.68/ 123.99	1827	-11.8	12/18 – 12/22/00
00-6	78.33/ 124.48	1639	-15.4	12/23 – 12/25/00
00-7	79.13/ 122.27	1494	-13.8	12/26 – 12/29/00
01-1	79.16/ 104.97	1843	-22.4	11/23 – 11/29/01
01-2	77.84/ 102.91	1353	-18.7	11/30 – 12/04/01
01-3	78.12/ 95.65	1633	-17.3	12/05 – 12/9/01
01-4	77.61/ 92.25	1484	-15.2	12/10 – 12/12/01
01-5	77.06/ 89.14	1246	-14.0	12/13 – 12/19/01
01-6	76.10/ 89.01	1232	-13.0	12/20 – 12/24/01
02-40	80.35/ 118.08	1537	-12.0	11/27 – 11/28/02
Byrd	80.02/ 119.60	1537	-13.8	11/28 – 12/7/02
02-1	82.00/ 110.01	1765	-18.1	12/8 – 12/13/02
02-2	83.50/ 104.99	1965	-24.1	12/13 – 12/17/02
02-3	85.00/ 105.00	2400	-24.0	12/19 – 12/22/02
02-4	86.50/ 107.99	2601	-24.4	12/23 – 12/27/02
02-5	88.00/ 107.98	2749	-23.8	12/27 – 12/30/02
South Pole	89.91/ 147.57	2810	-27.1	01/2 – 01/4/03

[a] average temperature during atmospheric chemistry measurements

Table 2. H_2O_2 mixing ratios measured during firn air experiments.

Site	time[a] (local noon)	duration, hrs	T_{air}[b] / SEA[c]	ambient air[d], pptv	firn air[d], pptv
01-5A	16-Dec-01 0:20 (17 :51)	4 :20	-7.4 / 35.9	756 ± 146	1442 ± 478
01-5B	16-Dec-01 20:10 (17 :51)	5:20	-11.4 / 35.9	783 ± 82	638 ± 74
02-1	10-Dec-02 23:59 (19 :13)	4:11	-17.0 / 30.9	416 ± 232	625 ± 52
02-2	16-Dec-02 1 :13 (18 :55)	5:00	-24.1 / 30.9	177 ± 32	128 ± 12
02-3	21-Dec-02 20:47 (18 :57)	4:33	-20.3 / 29.4	433 ± 61	888 ± 141
02-4A	26-Dec-02 1:41 (19 :11)	5 :00	-23.7 / 26.4	198 ± 36	257 ± 87
02-4B	26-Dec-02 6:58 (19 :11)	5 :40	-25.3 / 26.4	167 ± 53	245 ± 28
02-5	29-Dec-02 20:50 (19 :13)	5:39	-23.3 / 24.9	213 ± 158	742 ± 258

[a] median time of experiment

[b] mean air temperature during the experiment

[c] solar elevation angle in degrees

[d] mean and standard deviation for total length of experiment based on 2.5 min values

Table 3. Overview of environmental parameters during the inter comparison period in December 2000-2002; listed are averages and 1σ uncertainties.

Parameter	11/27 - 12/12/00	11/27 - 12/12/01	11/27 - 12/12/02
H_2O_2, ppbv	412±202	674±180	401±151
MHP, ppbv	-	314±129	403±161
latitude, °S	78.42 - 79.38	77.61 - 79.16	80.00 - 82.00
Elevation, m	1675 - 1791	1353 - 1843	1537 - 1765
air temperature, °C	-14.2±4.1	-19.0±3.8	-14.6±2.4
q_v, g kg^{-1}	-	0.72±0.21	1.13±0.14
wind speed, m s^{-1}	6.2±2.3	5.0±2.9	4.1±2.9
CO, ppbv	42.9±1.5	48.7±1.3	50.7±1.9
CH_4, pptv	1709±2	1708±2	1713±1
Surface O_3, ppbv	-	14.5±3.0	19.3±2.5
O_3 burden, DU	318±23	220±34	334±10
UV-B[a], W m^{-2}	0.35±0.33	0.60±0.55	0.30±0.26
UV-B[b], W m^{-2}	0.40±0.36	0.42±0.39	0.37±0.31

[a] calculated UV-B using observed ozone column densities

[b] calculated UV-B at constant ozone column densities (290 DU)

Figures

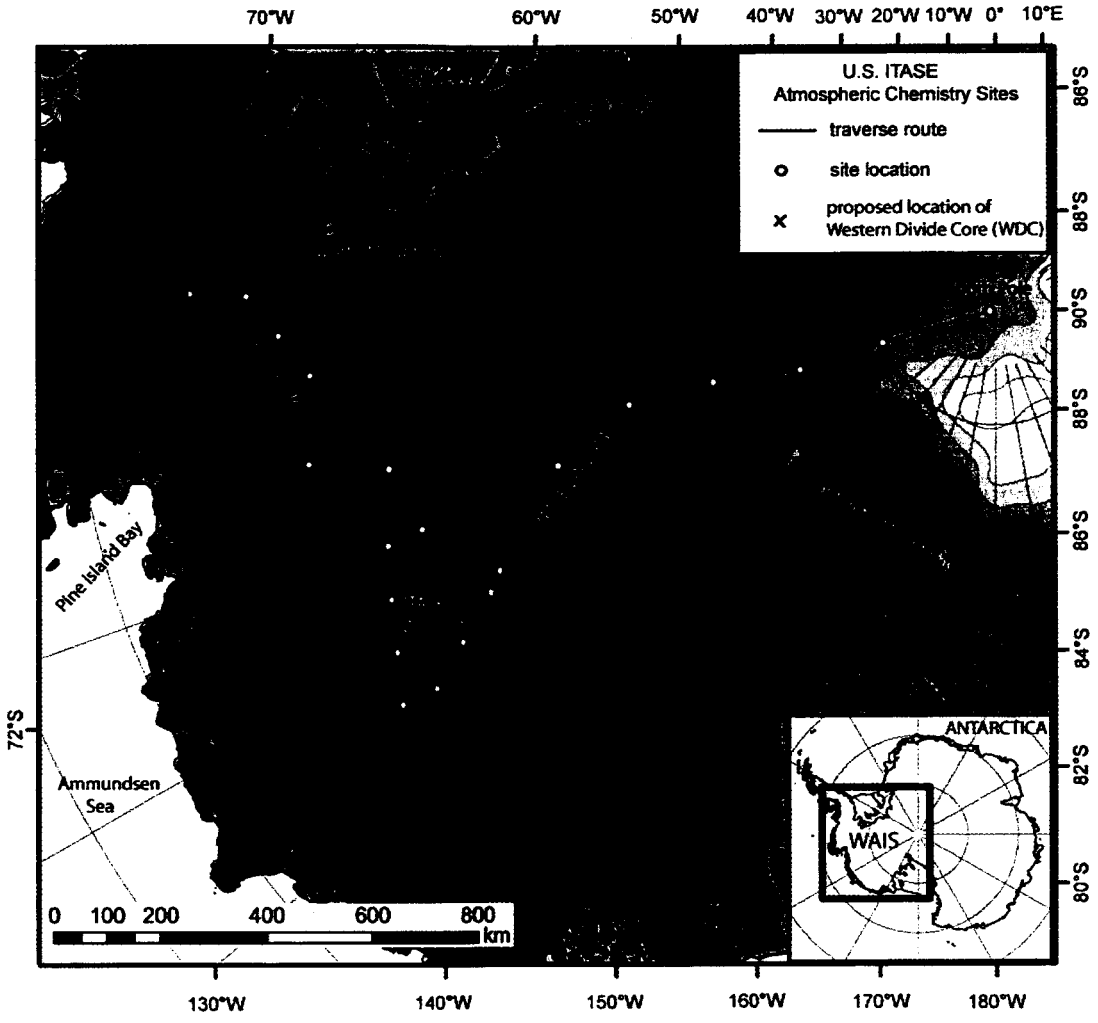

Figure 1. WAIS map (based on Antarctic Digital Data Base v4.1 http://www.add.scar.org/) overlying the RAMP DEM [*Liu, et al.*, 2001] showing traverse routes of the US component of the International Transantarctic Scientific Expedition (US ITASE; details of the multi-disciplinary expedition at http://www.ume.maine.edu/USITASE/) in 2000-2002 and the 21 locations of atmospheric chemistry observations.

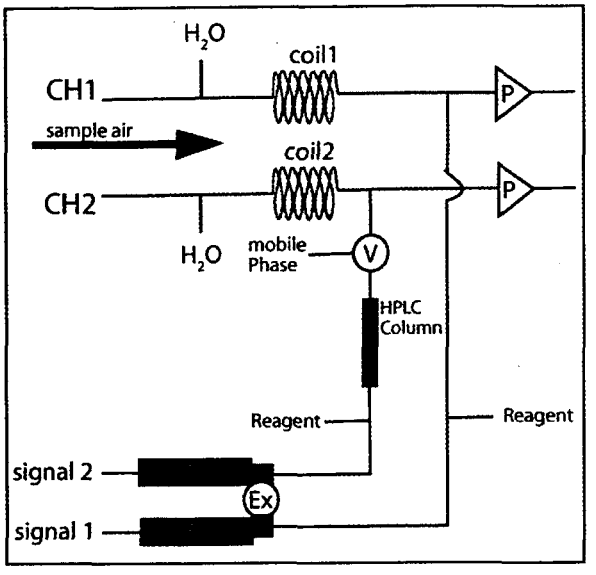

Figure 2. Schematic of 2-channel peroxide detector employed on ITASE; shown are air pumps (P), actuated injection valve (V), excitation source (Ex) and photo-multiplier tubes (PMT1 & 2).

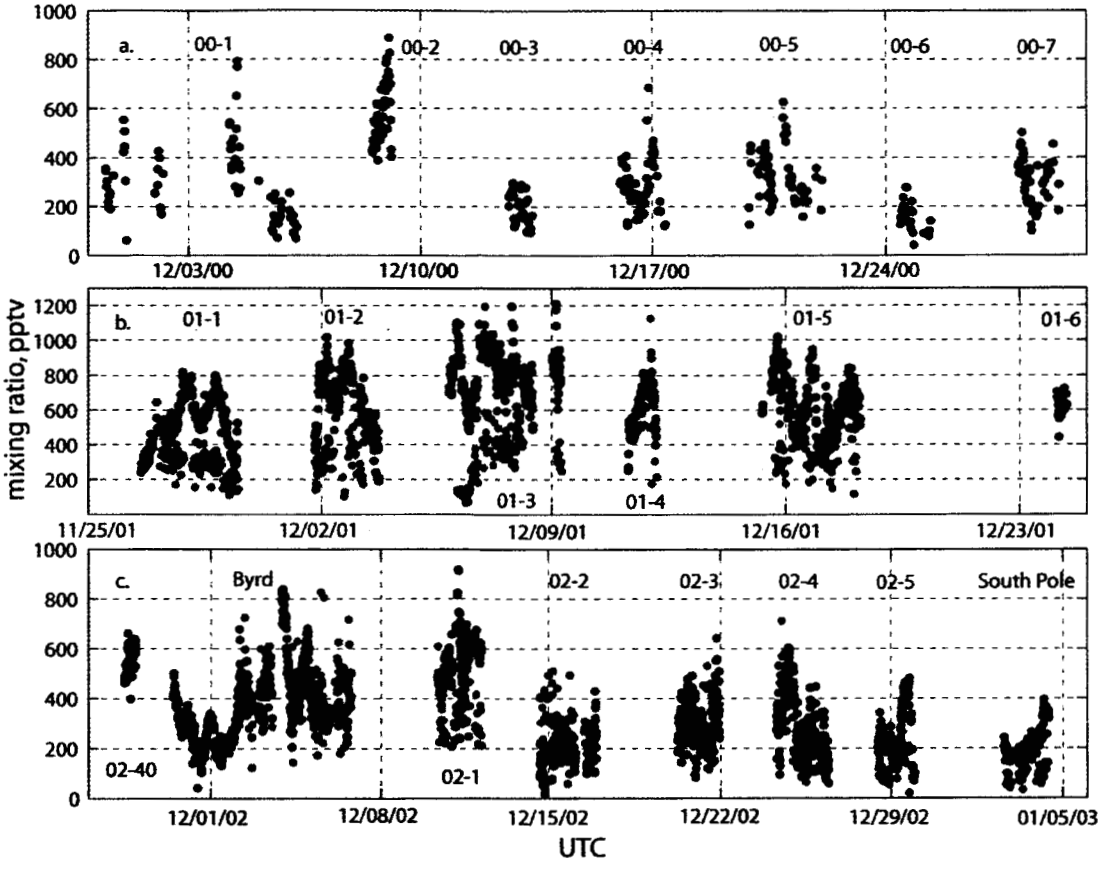

Figure 3. Mixing ratios of H_2O_2 (black symbols) and CH_3OOH (grey symbols) from 3 ITASE seasons observed during the month of December in 2000 (a.), 2001 (b.) and 2002 (c.). H_2O_2 is reported as 10 min averages, while the plotted MHP data represent single chromatograms, each one of them representing a ~5 min average of sampled air. Note that as the season progressed the measurement location changed as well, as indicated by the site index attached to each group of data. Data gaps are time periods when the ground traverse was in transition to a different site and no measurements were done.

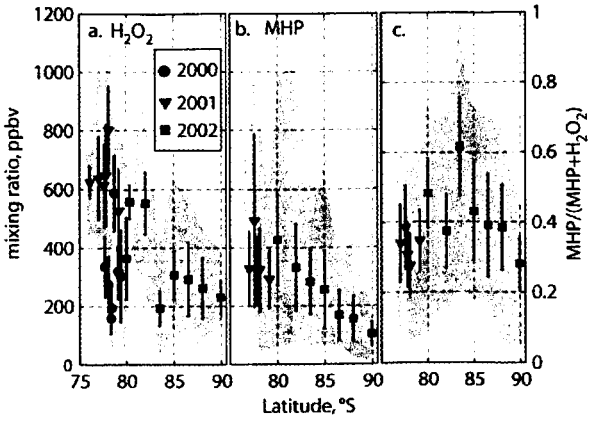

Figure 4. Site averages of atmospheric mixing ratios of H_2O_2 (a) and MHP (b) and ratios of MHP to total peroxide (c) as a function of latitude. Symbols are means with error bars indicating one standard deviation and shaded areas the full range of measurements.

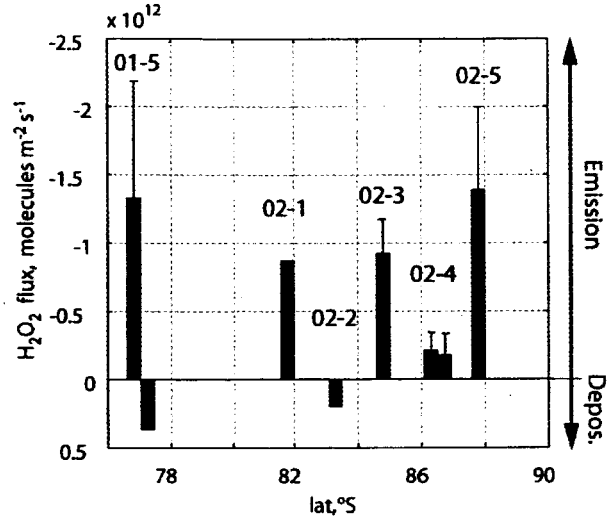

Figure 5. Estimates of H_2O_2 fluxes based on measured gradients between ambient and firn interstitial air are plotted as a function of latitude. Bars represent the mean and error bars 1 σ uncertainty. Note that at site 01-5 and 02-4 two sets of measurements are shown.

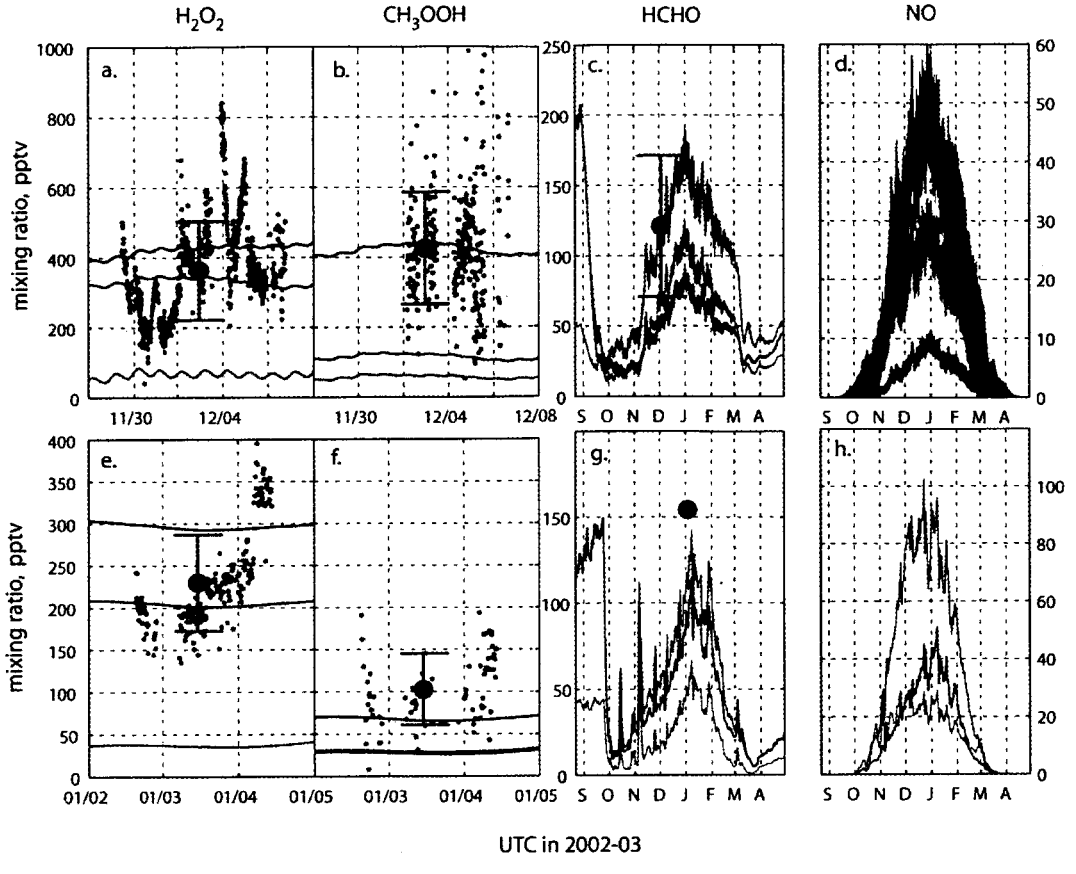

Figure 6. Comparisons between observations and photochemical box model estimates of atmospheric H_2O_2, MHP and HCHO mixing ratios for Byrd (a-c) and South Pole (e-g). Calculated NO background values are plotted as well for both sites (d,h). Various model scenarios include: 1) a base case with standard reaction rates and no heterogeneous fluxes for ROOH and HCHO (grey lines) and 2) multiple runs with reaction rates optimized for MHP production, emission fluxes of H_2O_2 and HCHO included and the NO source set for different backgrounds in December (blue and red lines). Black symbols are observed mean concentrations at each site with error bars indicating the 1σ uncertainty range, while symbols in grey represent 10 min averages of measured H_2O_2 and MHP. No DNPH results were available from South Pole, instead one 24 hr run from site 02-5 was used for comparison with no uncertainty range (g).

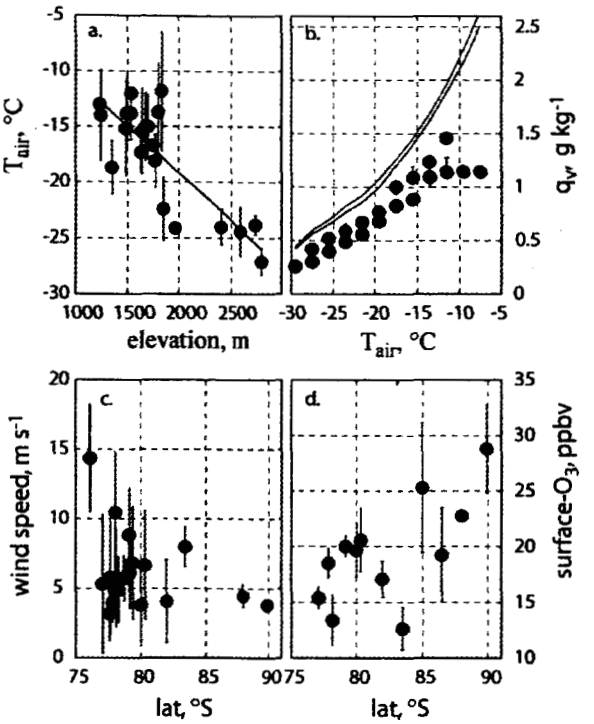

Figure 7. Correlation plots of observed and calculated environmental parameters on ITASE: a. air temperature vs. elevation with the black line illustrating the linear trend (slope –8.45 K/m, r^2 = 0.67), b. observed specific humidity q_v (symbols and error bars correspond to median, 25th and 75th percentile of each bin) vs. air temperature. Also shown is potential q_v at RH=100% (25th and 75th percentile as grey lines), c. wind speed vs. latitude and d. surface ozone vs. latitude. Symbols and error bars in a., c. and d. represent mean and 1σ uncertainty at each site and individual field seasons are color coded: ITASE 2000 (blue), ITASE 2001 (black) and ITASE 2002 (red). All meteorological and surface ozone data used are 10 min averages from December/January of the respective year (note that neither humidity nor surface ozone were measured in 2000).

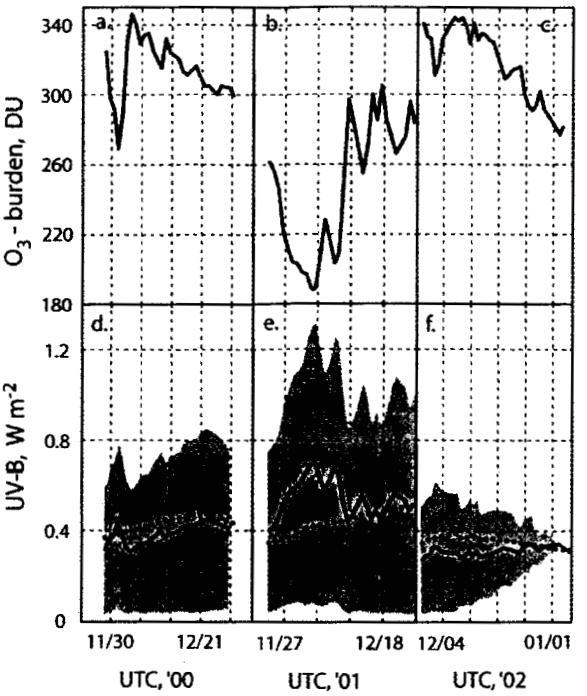

Figure 8. Panels a-c show daily ozone column densities from TOMS during each field season above the location of the ITASE traverse on the same dates. Panels d-f show calculated surface UV-B (280-315 nm), where the black line represents daily means and the area shaded in grey illustrates the amplitude between solar noon and midnight; surface UV-B radiation was also calculated for ozone column densities fixed at a constant 290 DU (dotted black line).

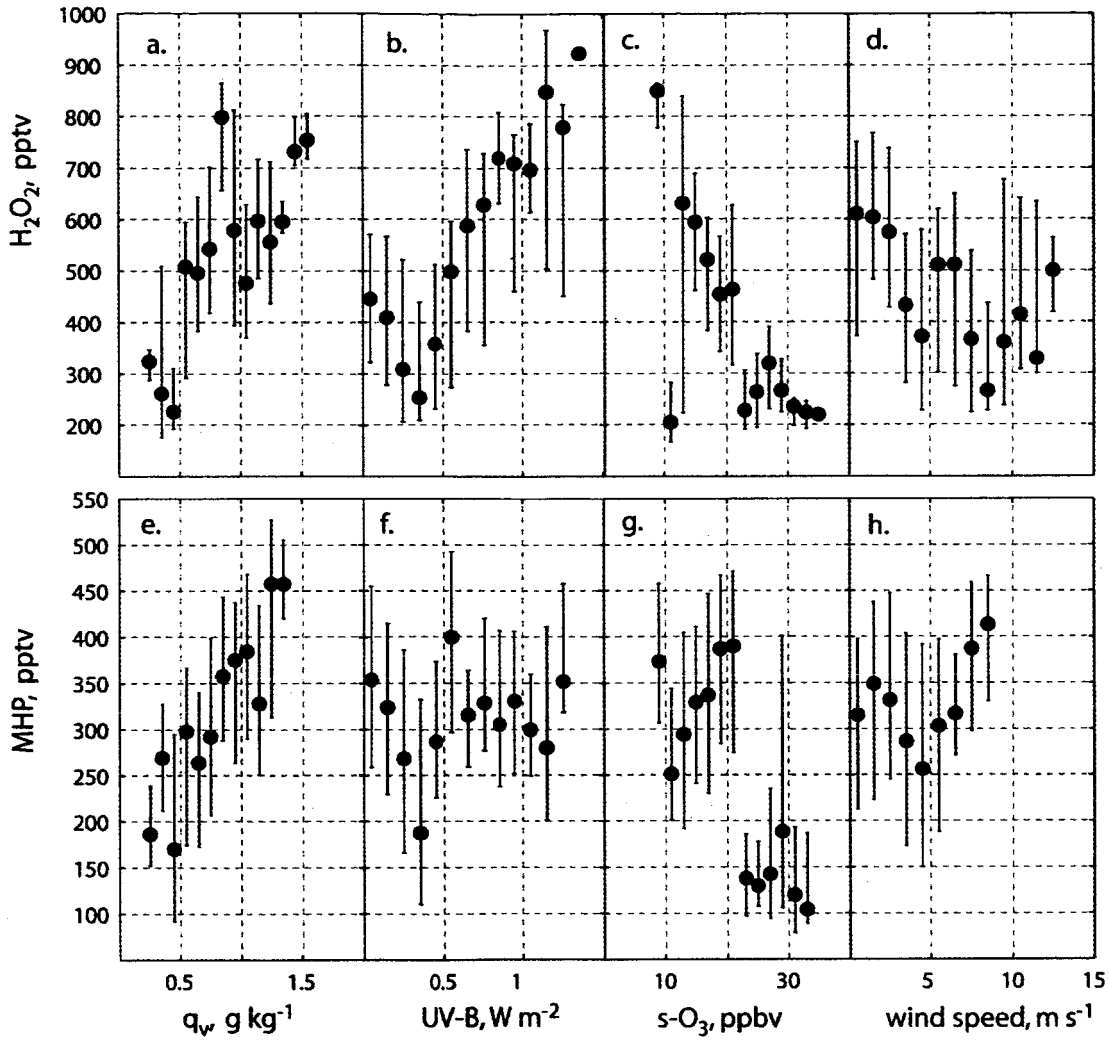

Figure 9. Correlation plots of binned ROOH observations: (a./.e) H_2O_2/MHP vs. specific humidity q_v, (b./f.) H_2O_2/MHP vs. calculated surface UV-B radiation (280-315 nm), (c./g.) H_2O_2/MHP vs. surface ozone and (d./h.) H_2O_2/MHP vs. wind speed. Symbols and error bars represent median values and inner quartiles (25th and 75th percentiles). All data used are 10 min averages in December 2001, 2002 and early January 2003 (wind speed and UV-B correlation plots contain also December 2000 data).

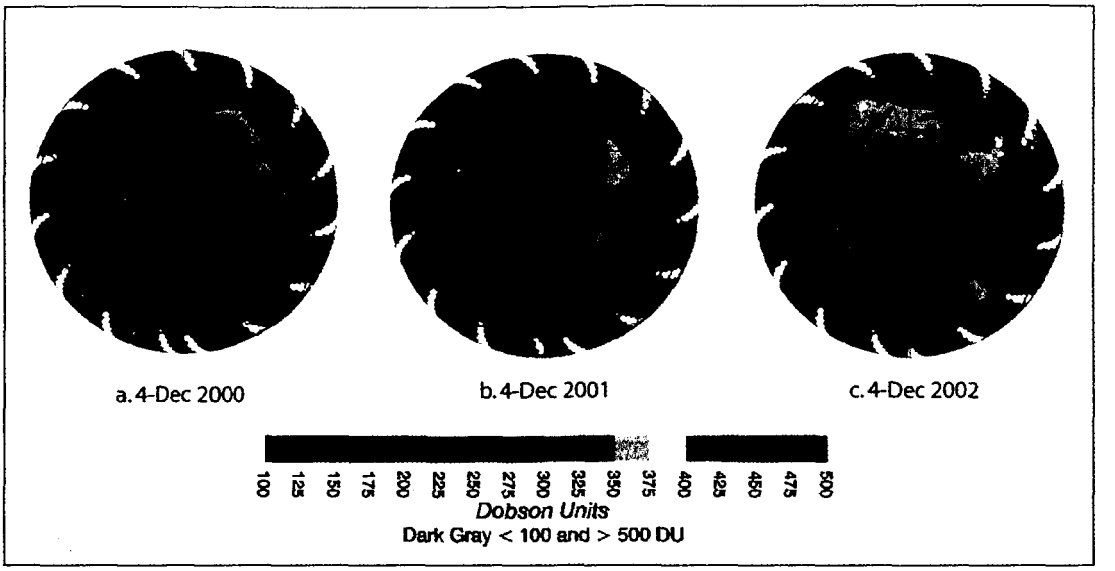

Figure 10. Spatial distributions of total ozone above Antarctica are compared between December 2000 (Panel a.), 2001 (Panel b.) and 2002 (Panel c.). Images show data recovered by the Earth Probe TOMS instrument (http://toms.gsfc.nasa.gov/ozone). White areas represent data gaps.

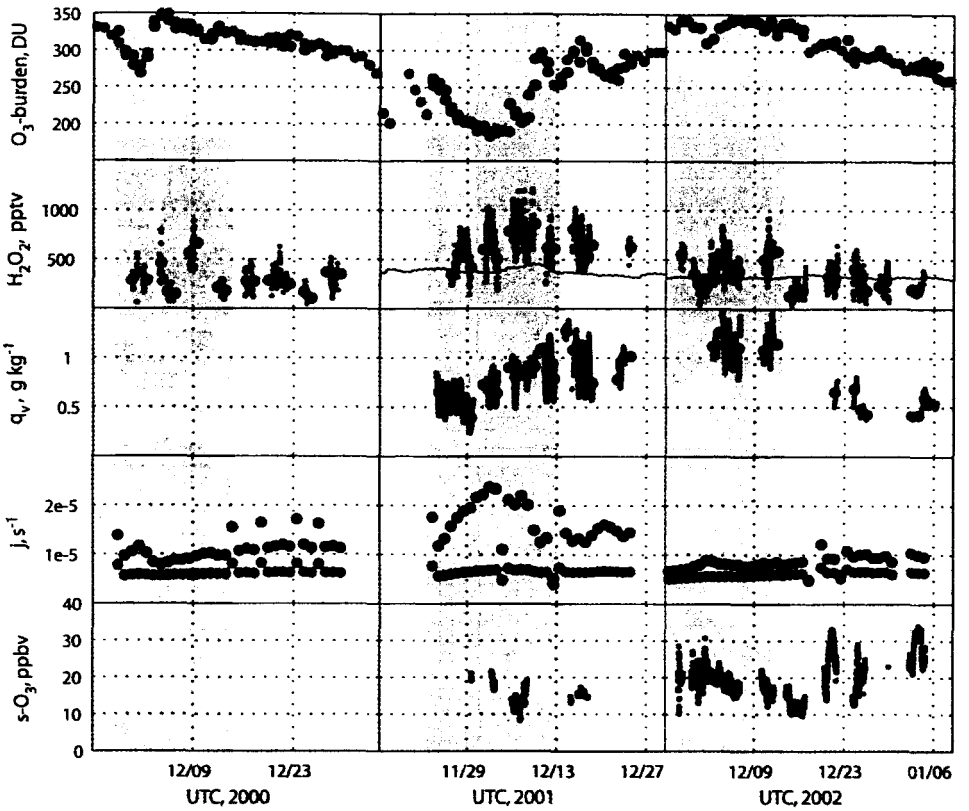

Figure 11. Atmospheric H_2O_2 and related parameters are shown from 2000, 2001 and 2002, each column representing one season of measurements. Areas shaded in grey highlight the comparison period November-27 - December-12 (Table 3). In row 1 daily column densities of ozone are plotted against time (grey symbols represent Byrd, while the black symbols take into account the current position of the ITASE traverse on the ice sheet). The second row shows 10 minute (grey symbols) and 24 hour averages (black symbols) of observed H_2O_2. Plotted are also simulated H_2O_2 mixing ratios in 2001 and 2002 from the optimized fit to observations at Byrd in 2002 (black line). The third row illustrates the variability of specific humidity (10 minute and 24 hr averages plotted as grey and black symbols, respectively; no data available from 2000). Calculated daily averages of photolysis rates for O_3 (black symbols) and H_2O_2 (grey symbols) are shown in the fourth row, and surface O_3 measurements from ITASE2001 and 2002 are plotted in the fifth row.

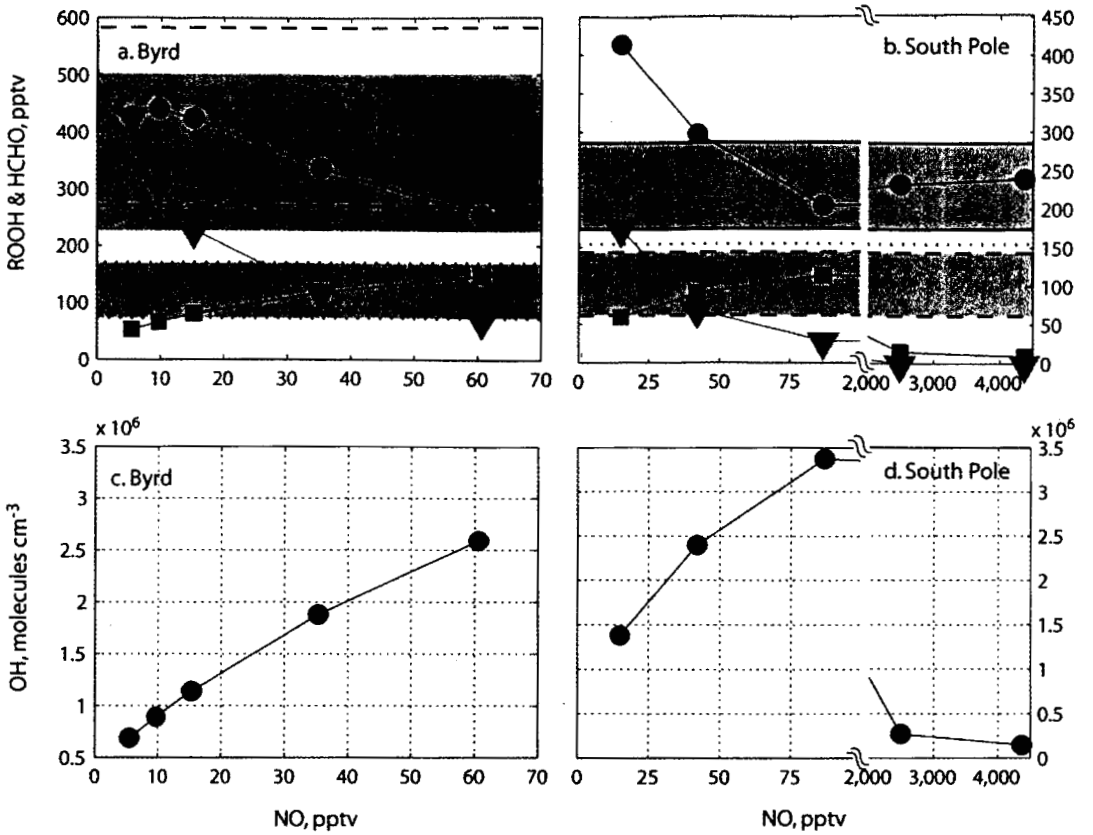

Figure 12. Sensitivities of calculated H_2O_2, CH_3OOH and HCHO to increasing NO background levels are shown for a. Byrd (29.11.02-7.12.02) and b. South Pole (2.01.03-5.01.03). Symbols represent output of individual box model runs for H_2O_2 (circles), MHP (grey triangles) and HCHO (squares). Observation ranges, defined as the mean plus and minus 1σ, are shown as shaded areas with solid, broken and dotted border lines for H_2O_2, CH_3OOH and HCHO respectively. Note that at South Pole only one data point for HCHO is available (see text). Panels c. and d. illustrate the relationship across the same model runs between calculated NO and OH radical concentrations at Byrd and South Pole.

Popular Summary

The troposphere above the West Antarctic Ice Sheet (WAIS) was sampled for hydroperoxides at 21 locations during 2-month-long summer traverses from 2000 to 2002, as part of US ITASE (International Transantarctic Scientific Expedition). First time quantitative measurements using an HPLC method showed that methylhydroperoxide (MHP) is the only important organic hydroperoxide occurring in the Antarctic troposphere, and that it is found at levels ten times those previously predicted by photochemical models. During three field seasons, means and standard deviations for hydrogen peroxide (H_2O_2) were 321±158 pptv, 650±176 pptv and 330±147 pptv. While MHP was detected, but not quantified in December 2000, levels in summer 2001 and 2002 were 317±128 pptv and 304±172.2 pptv. Results from firn air experiments and diurnal variability of the two species showed that atmospheric H_2O_2 is significantly impacted by a physical snow pack source between 76 and 90 °S, whereas MHP is not. We show strong evidence of a positive feedback between stratospheric ozone and H_2O_2 at the surface. Between November-27 and December-12 in 2001, when ozone column densities dropped below 220 DU (means in 2000 and 2001 were 318 DU and 334 DU, respectively), H_2O_2 was 1.7 times that observed in the same period in 2000 and 2002, while MHP was only 80% of the levels encountered in 2002. Photochemical box model runs suggest that NO and OH levels on WAIS are closer to coastal values, while Antarctic Plateau levels are higher, confirming that region to be a highly oxidizing environment. The modeled sensitivity of H_2O_2 and particularly MHP to NO offers the potential to use atmospheric hydroperoxides to constrain the NO background and thus estimate the past oxidation capacity of the remote atmosphere.